The Plant Cell, Vol. 18, 3502–3518, December 2006, www.plantcell.org

Somatic Cytokinesis and Pollen Maturation in *Arabidopsis* Depend on TPLATE, Which Has Domains Similar to Coat Proteins [W]

Daniël Van Damme, Silvie Coutuer, Riet De Rycke, Francois-Yves Bouget,[1] Dirk Inzé, and Danny Geelen[2,3]

Department of Plant Systems Biology, Flanders Interuniversity Institute for Biotechnologie, Ghent University, B-9052 Gent, Belgium

TPLATE was previously identified as a potential cytokinesis protein targeted to the cell plate. Disruption of TPLATE in *Arabidopsis thaliana* leads to the production of shriveled pollen unable to germinate. Vesicular compartmentalization of the mature pollen is dramatically altered, and large callose deposits accumulate near the intine cell wall layer. Green fluorescent protein (GFP)–tagged TPLATE expression under the control of the pollen promoter Lat52 complements the phenotype. Downregulation of *TPLATE* in *Arabidopsis* seedlings and tobacco (*Nicotiana tabacum*) BY-2 suspension cells results in crooked cell walls and cell plates that fail to insert into the mother wall. Besides accumulating at the cell plate, GFP-fused TPLATE is temporally targeted to a narrow zone at the cell cortex where the cell plate connects to the mother wall. TPLATE-GFP also localizes to subcellular structures that accumulate at the pollen tube exit site in germinating pollen. Ectopic callose depositions observed in mutant pollen also occur in RNA interference plants, suggesting that TPLATE is implicated in cell wall modification. TPLATE contains domains similar to adaptin and β-COP coat proteins. These data suggest that TPLATE functions in vesicle-trafficking events required for site-specific cell wall modifications during pollen germination and for anchoring of the cell plate to the mother wall at the correct cortical position.

INTRODUCTION

The cell wall of higher plant cells provides the mechanical strength required to hold the structure of the entire plant body. New walls are laid down after mitosis through the activity of a cytoskeletal configuration known as the phragmoplast. The immature wall or cell plate emerges first at the cell center from deposits that travel along microtubules to the spindle midzone. In the next step, the young disk-shaped plate expands outward until it reaches the cellular boundaries and unites with the existing mother wall (for review, see Jürgens, 2005a, 2005b). Positioning of the new cell wall after mitosis is critical for the establishment of the cellular organization of plant tissues and the overall morphology of the plant (Lloyd, 1995; Traas et al., 1995). Plants have developed regulatory mechanisms to position and guide the new cell plate. Two plant-specific microtubular arrays are involved in the positioning and guidance of the new cell plate, the preprophase band (PPB) and the phragmoplast itself. The PPB consists of a ring of microtubules and actin filaments, encircles the nucleus at prophase, and determines the future division zone (Mineyuki and Gunning, 1990; Wick, 1991; Mineyuki, 1999). The PPB is removed before chromosome segregation and cytokinesis and therefore cannot contribute directly to the cell plate guidance process. As the PPB microtubules degrade, cortical actin at the corresponding former position of the PPB disappears, leaving behind a zone devoid of actin filaments (Cleary et al., 1992; Sano et al., 2005). The role of actin in cytokinesis is not very clear. Actin depolymerization slows mitotic progression and affects phragmoplast initiation. However, it does not have a major impact on cell plate positioning (Yoneda et al., 2004). Recently, a novel marker was identified that implicates the plasma membrane as an additional structure that may be important for determining the division zone (Vanstraelen et al., 2006). The marker is a green fluorescent protein (GFP)–tagged kinesin, KCA1, which associates with the plasma membrane at the onset of mitosis. It is excluded from a region corresponding to the size and position of the PPB and the actin-depleted zone. By analogy, it was called the KCA-depleted zone or KDZ. The KDZ persists throughout mitosis until the new cell plate has expanded to reach the mother wall and therefore marks the division zone. It remains to be investigated whether KCA1 plays a direct role in the positioning and guidance of the cell plate.

The phragmoplast is required to construct the new cell plate and conducts guidance of the plate to the division zone. The double array of parallel-oriented microtubules of the phragmoplast transport Golgi- or endosome-derived vesicles, containing cell plate–building blocks, to the equatorial plane of the cell, where they

[1] Current address: Laboratoire Arago, Unité Mixte de Recherche 7628, Centre National de la Recherche Scientifique, Université Pierre et Marie Curie, B.P. 44, F-66651 Banyuls sur Mer cedex, France.
[2] Current address: Department of Plant Production, Faculty of Bioscience and Bioengineering, Ghent University, Coupure Links 653, B-9000 Gent, Belgium.
[3] To whom correspondence should be addressed. E-mail danny.geelen@ugent.be; fax 32-9-264-62-25.
The author responsible for distribution of materials integral to the findings presented in this article in accordance with the policy described in the Instructions for Authors (www.plantcell.org) is: Danny Geelen (danny.geelen@ugent.be).
[W] Online version contains Web-only data.
www.plantcell.org/cgi/doi/10.1105/tpc.106.040923

immediately fuse and give rise to a tubulovesicular network. Callose deposition inside the lumen of the network may provide a spreading force for the widening of the tubular network and convert it to a fenestrated sheet (Samuels et al., 1995). Fusion of the cell plate with the plasma membrane triggers a maturation process that involves the replacement of callose by cellulose. The mechanism and controlling elements required for the switch from a callose- to a cellulose-containing cell plate are still unknown. Mutants that are altered in cellulose biosynthesis often show cytokinesis defects: *cyt1* (Nickle and Meinke, 1998; Lukowitz et al., 2001), *prc1* (Fagard et al., 2000), *kor1*/*rsw2* (Zuo et al., 2000; Lane et al., 2001), *kob1* (Pagant et al., 2002), and *fk*, *hyd1*, and *smt1*/*cph* (Schrick et al., 2000). The cytokinesis defects described for *cyt1*, *kob1*, *prc1*, *fk*, *hyd1*, and *smt*/*cph* can be attributable to impeded wall formation that is manifested by disrupted cell walls in microscopic sections. The *kor1-2* mutant produces, in addition to cell wall stubs, curved and misplaced cell walls, despite the fact that the PPB is correctly positioned in these cells (Zuo et al., 2000). *korrigan* (*kor1-2*) is an endo-1,4-β-glucanase, indicating that factors that are not linked directly to PPB activity are also required for the correct guidance of the cell plate.

Ultimately, cell plate expansion results in a fusion with the existing wall. From a mechanistic viewpoint, the cell plate inserts in the mother wall through a multitude of finger-like fusion tubes that contact the parental plasma membrane in the zone of adhesion (Samuels et al., 1995). Because the cell plate membrane and the plasma membrane are at first independent structures, their unification must rely on a membrane fusion process that involves membrane fusion machinery different from the KNOLLE/KEULE/SNAP33 SNARE complex that is required for cell plate formation and expansion (Jürgens, 2005a). To date, there is little information on the components that contribute to the anchoring of the plate to the mother wall. A candidate protein is ROOT/SHOOT/HYPOCOTYL-DEFECTIVE (RSH), a hydroxyl Pro-rich glycoprotein (extensin) that accumulates at the site of cell plate–cell wall contact. Disruption of the RSH protein is embryo-lethal and causes misplaced cell plates, resulting in irregular cell shape and size (Hall and Cannon, 2002).

Here, we report the functional analysis of *TPLATE*, a gene with a role in cell plate anchorage. TPLATE-GFP (previously T22-GFP) localizes to the midline of the expanding phragmoplast in dividing tobacco (*Nicotiana tabacum*) BY-2 cells (Van Damme et al., 2004a). During the final steps of cell plate expansion, GFP-fused TPLATE accumulates at a defined zone of the plasma membrane that corresponds to the division zone. TPLATE-GFP also accumulates at the pollen tube exit site during pollen germination, in agreement with the male-sterility phenotype that is caused by a T-DNA insertion in *TPLATE*. How cytokinesis and pollen development are connected is inferred from the similarity of TPLATE and vesicle-associated proteins, suggesting a role in heterotypic vesicle fusion.

RESULTS

TPLATE Is Similar to Coat Proteins

A GFP-based screen in BY-2 cells identified TPLATE (clone T22) as a putative cell plate–targeted protein (Van Damme et al., 2004a). To analyze the relevance of this gene to other species, the occurrence of homologous sequences was determined (Figure 1). *TPLATE* is unique to plant species and occurs as a singleton located on chromosome 3 in *Arabidopsis thaliana*. There are two copies in rice (*Oryza sativa* var *japonica*), one on chromosome 11 (Os11g07470) and one on chromosome 2 (Os2g55010). *Arabidopsis TPLATE* and the rice homologs exhibit a genomic structure of seven exons and six introns (Figure 2). The *Arabidopsis* TPLATE is ~70% identical to the rice homologs and 82% identical to a predicted protein sequence from *Lotus corniculatus* var *japonicus* (AP004906). A partial EST sequence (translated 160 amino acids) from *Physcomitrella patens* (BJ187435) is 57% identical (79% similar), indicating that the protein is highly conserved from mosses to higher plants. The *TPLATE* open reading frame predicts a protein with a molecular mass of 131 kD and contains domains with similarity to an EF-hand motif (IPR002048) and an adaptin_N domain (IPR002553), as identified by standard analysis (www.sanger.ac.uk/cgi-bin/pfam; Figure 2A). The adaptin_N domain is present in the N-terminal part of the large subunits of the AP-1, AP-2, AP-3, and AP-4 adaptor protein complexes and in the β-COP, γ1-COP, and γ2-COP subunits of the COPI protein complex (Boehm and Bonifacino, 2001). Adaptin protein complexes (AP) and coat protein complexes (COP) are involved in clathrin-coated and non-clathrin-coated vesicle formation (McMahon and Mills, 2004). Besides an adaptin_N-like domain, TPLATE carries a stretch of 14 amino acids highly

At3g01780|TPLATE	772 - **PLTGSSDPCYIEAY** - 785
XP_46823| Oryza sativa japonica	770 - **SLTGSSDPCYIEAY** - 783
AAX95799.1|Oryza sativa japonica	770 - **TLTGSSDPCYIEAY** - 783
AP004906.1|Lotus corniculatus japonicus	770 - **TLTGSSDPCYVEGY** - 783
At4g31480|Arabidopsis Beta-cop	742 - **QLTGFSDPVYAEAY** - 755
At4g31490|Arabidopsis Beta-cop	718 - **QLTGFSDPVYAEAY** - 732
P23514|COPB_RAT	718 - **QLTGFSDPVYAEAY** - 731
Q23924|COPB_DICDI	166 - **QLSGFSDPIYVEAY** - 179
Q9JIF7|COPB_MOUSE	718 - **QLTGFSDPVYAEAY** - 731
P53618|COPB_HUMAN	718 - **QLTGFSDPVYAEAY** - 731
P45437|COPB_DROME	731 - **QLTGFSDPVYAEAY** - 744
NP_913038.1|O. sativa japonica Beta-cop	807 - **QLTGFSDPVYAEAY** - 820
NP_494441.1|C. elegans coatomer protein	727 - **QLAGFSDPIYAEAY** - 740

Figure 1. Alignment of the β-COP–Specific Element.

A stretch of 14 amino acids (the β-COP–specific element) is conserved in β-COP and TPLATE. Conserved amino acids in β-COP proteins derived from different species are shown in boldface. Numbers represent the amino acid positions of the element within the proteins.

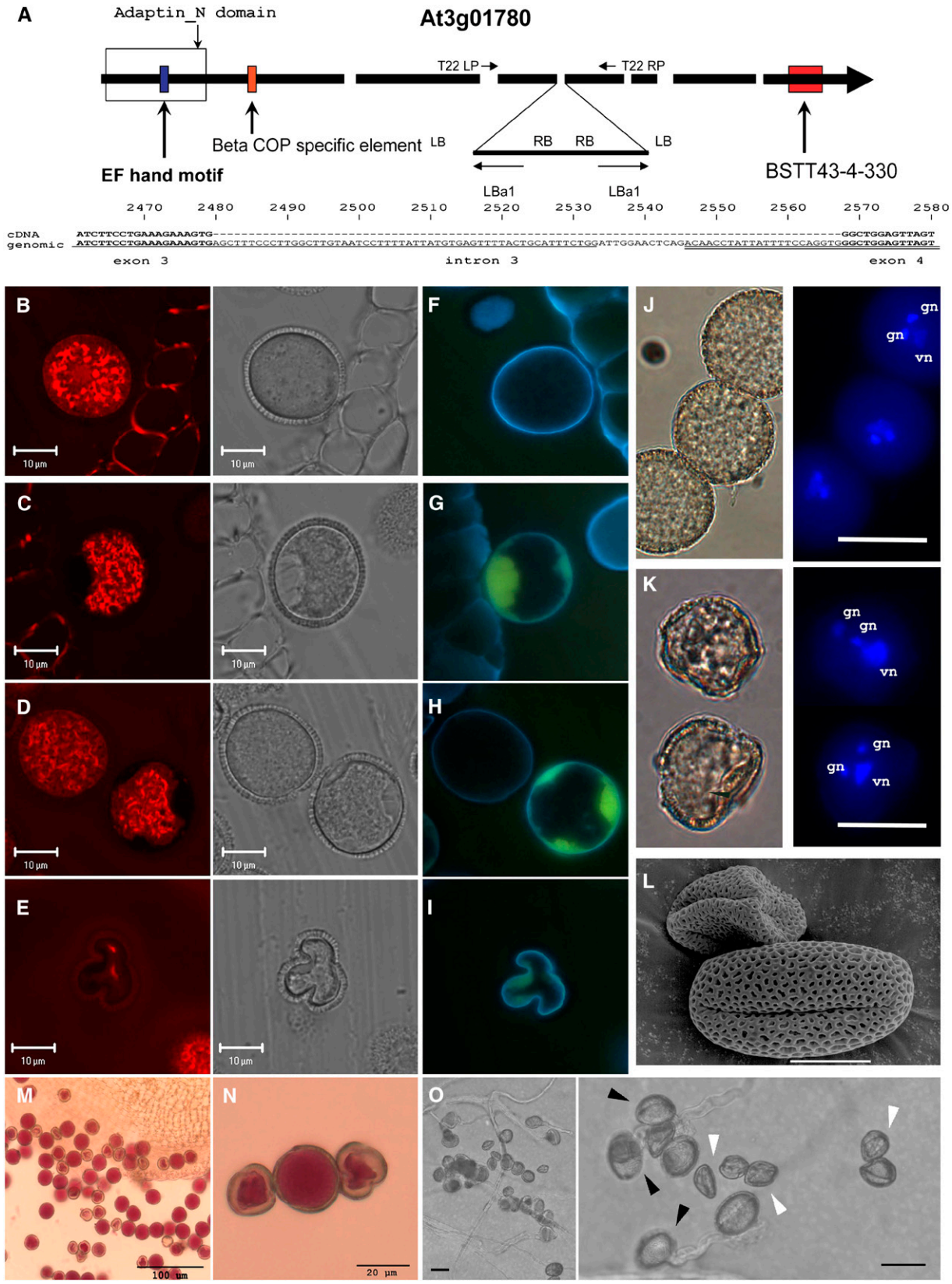

Figure 2. Analysis of *tplate* Mutant Pollen.

conserved in β-coatomer proteins (β-COP). We called this motif the β-COP–specific element (Figure 1). The composition of the motif was determined as [P]L[T]G-[S]-SDP-x-Y-x-E[AY], with x indicating any amino acid and amino acids in brackets partially conserved in the β-COP protein family. The β-COP–specific element is conserved in β-COP proteins across the different genera (Figure 1). The occurrence of a β-COP element and a domain similar to adaptin_N in TPLATE suggests that the TPLATE protein is related to coat proteins.

A T-DNA Insertion in TPLATE Causes Complete Male Sterility

TPLATE is interrupted at the third intron by a T-DNA insertion in the *Arabidopsis* line SALK_003086 (Figure 2A). Sequences adjacent to the insertion site are amplified by PCR with the T-DNA left border primer (LBaI) and primers of neighboring sequences (T22-RP and T22-LP), suggesting that the insertion is an inverted repeat. Determination of the T-DNA–bordering sequences confirmed the presence of two left borders and identified the exact position of the insertion site (Figure 2A). Segregation analysis of heterozygous plants resulted in 50% progeny showing resistance to kanamycin. All kanamycin-resistant plants ($n = 30$) were heterozygous for the T-DNA insertion. PCR on a population of plants that were grown without selection also yielded the 1:1 segregation ratio (131 heterozygous and 151 wild-type plants; χ^2 test for a 1:1 ratio yields 1.42, and χ^2 95% interval value is 3.84). Pollination of wild-type plants with pollen from the *TPLATE* heterozygous mutant resulted solely in kanamycin-sensitive plants (72 plants tested), indicating that the mutation cannot be passed on by the male gametophyte and that the T-DNA insertion in *TPLATE* affects pollen development or germination. By contrast, the insertion mutation has no discernible effect on the development of the female gametophyte, as seed setting and yield were similar to those of wild-type plants (data not shown).

tplate Mutant Pollen Shows Normal Karyokinesis and Is Defective in a Late Developmental Stage

The development of the male gametophyte was analyzed using light and fluorescence microscopy. Pollen produced by a heterozygous *tplate* mutant plant is shown in Figure 2. Dehiscing anthers were stained with Alexander's stain to discriminate between live and dead pollen. The cytoplasm of viable pollen becomes brightly red, whereas dead pollen is not stained by the dye (Alexander, 1969). Two types of pollen grains were observed: wild-type pollen that is oval-shaped, and shriveled, irregularly shaped mutant pollen (Figures 2M and 2N). The ratio between irregular and normal pollen was 1:1 (532 mutant and 526 wild-type grains; χ^2 test for a 1:1 ratio yields 0.03, and χ^2 95% interval value is 3.84). The cytoplasm of the mutant pollen grains stained red with the Alexander stain, indicating that the pollen is not dead at this stage. Yet, some of the pollen had collapsed and showed a thick layer of translucent deposit against the pollen intine wall (Figure 2N).

To determine the developmental stage and nuclear composition of the pollen, dehiscing anthers were stained with 4′,6-diamidino-2-phenylindole (DAPI). Wild-type (Figure 2J) and mutant (Figure 2K) pollen carried three nuclei, two male gamete nuclei and one vegetative nucleus, indicating that nuclear divisions occurred during pollen development. Observation of earlier stages in pollen development did not reveal morphological differences and tetrads, as ring-vacuolated, bicellular, and early trinucleate pollen appeared as in wild-type plants, suggesting that the mutation affects later stages of pollen maturation (data not shown). To assess the germination capacity of wild-type versus mutant pollen grains, anthers were spread on germination medium and observed after 8 and 16 h of incubation. In a control experiment, 80% of wild-type pollen germinated. Pollen derived from anthers harvested from mutant plants showed a reduction of germination capacity of ~50%, and none of the shriveled pollen germinated (Figure 2O).

Callose Accumulates Ectopically in Mutant Pollen Grains

The thick deposits at the cell periphery in mutant pollen grains may have prevented germination by changing the structure of the intine wall layer. To determine the structure and composition of the mutant pollen cell wall, sections of plastic-embedded whole-mount anthers were stained with fluorescent cell wall dyes. Propidium iodide (PI) treatment identified three

Figure 2. (continued).

(A) *TPLATE* gene structure with indication of domains, the T-DNA insertion position, and the position of the tobacco cDNA AFLP tag (BSTT43-4-330) used for RNAi in BY-2 cells. Arrows indicate primers (Lba1, T22 LP, and T22 RP) used to check the T-DNA insertion. Sequence information obtained by sequencing the fragments (T22 LP–Lba1 [underlined] and T22 RP–Lba1 [double underlined] primer pairs) identifies the T-DNA insertion within the third intron and confirms the inverted repeat T-DNA structure.

(B) to **(E)** Confocal images of thin sections through anthers of a *TPLATE* heterozygous plant. Thin sections (5 μm) were stained with PI. Mutant pollen in images **(C)** and **(D)** show inclusions not stained by PI. **(E)** shows a shriveled pollen grain.

(F) to **(I)** Epifluorescence images of thin sections, costained with calcofluor white (blue) and aniline blue (yellow), showing a wild-type pollen grain **(F)** and callose depositions (**[G]** to **[I]**) inside the mutant pollen of images **(B)** to **(E)**.

(J) and **(K)** Epifluorescence images of wild-type **(J)** and mutant **(K)** pollen stained with DAPI. Mutant pollen is trinucleate. gn, gamete nucleus; vn, vegetative nucleus. Bars = 20 μm.

(L) Scanning electron micrograph of mutant and wild-type pollen grains. Bar = 10 μm.

(M) and **(N)** Bright-field microscope images showing an overview **(M)** and a close-up **(N)** of wild-type and mutant pollen grains visualized with Alexander's stain. Bars = 100 μm in **(M)** and 20 μm in **(N)**.

(O) Germinating pollen grains. Normal-looking pollen germinates (black arrowheads), in contrast with the mutant pollen (white arrowheads). Bars = 20 μm.

types of pollen grains. Fifty percent of the pollen grains had a normal ellipsoidal morphology and fluoresced homogenously (Figure 2B). The other half of the pollen grains showed random deposits of material that was not stained by PI (Figures 2C and 2D). In severely affected pollen with a shriveled appearance, there was no PI staining (Figure 2E). This type of pollen occurred more frequently in mature anthers and probably represents an end stage in the maturation of the mutant pollen. The deposits were also observed in the representative bright-field images (Figures 2C and 2D). The deposits occurred mostly at the cell periphery; therefore, the intine cell wall composition was analyzed using calcofluor white and aniline blue staining methods. A mixture of aniline blue and calcofluor white distinctively labels callose (yellow fluorescence) and cellulose (blue-green fluorescence), respectively (Figures 2F to 2I) (Jefferies and Belcher, 1974). The wild-type intine cell wall was predominantly composed of cellulose and stained brightly blue with calcofluor (Figure 2F). The intine wall from shriveled pollen (Figures 2G to 2I) was fluorescent in the presence of calcofluor white, albeit less pronounced than in wild-type grains. Hardly any aniline blue fluorescence occurred in wild-type pollen (Figure 2F) because very little callose was present in these cells. By contrast, brightly yellow fluorescent spots occurred in mutant pollen (Figures 2G to 2I).

To analyze the deposits in more detail, pollen morphology was determined by means of scanning and transmission electron microscopy. The scanning images revealed that the exine layer of mutant pollen is similarly structured as in wild-type pollen (notice that the mutant pollen grain is approximately half the size of the wild-type pollen grain; Figure 2L). Transmission electron microscopic analysis further confirmed that the structure and organization of the exine are normal. Figure 3A shows an overview of an ultrathin section of a mutant and a wild-type pollen grain. Wild-type mature pollen is densely packed with vesicles, endoplasmic reticulum, and Golgi (Figures 3B and 3E). At the periphery, a band of Pb acetate–stained vesicles concentrates adjacent to the intine layer. Closer to the center, there are more electron-dense (dark) vesicles mixed with less numerous (electrolucent) vesicles (Figure 3B). The peripheral vesicles are presumably involved in secreting polysaccharide cell wall components upon germination and subsequent pollen tube growth (Heslop-Harrison, 1987). Mature mutant pollen grains show an altered composition of the pollen cytoplasm with small and large electron-dense bodies (Figures 3B and 3H). The composition of the cytoplasm in not fully matured mutant pollen with less severe morphological deformations shows an intermediate stage with undulations of the plasma membrane (arrows in Figures 3C and 3G). Using a specific antibody directed against callose, strong labeling was detected specifically between the intine cellulose layer and the undulated plasma membrane (Figure 3D), whereas hardly any signal was detected in mature wild-type pollen (Figure 3F). The altered composition of the mature mutant pollen grains compared with wild-type pollen, together with the undulations of the plasma membrane, suggest a defect in the regulation of the plasma membrane surface in the mutant pollen. The failure of mutant TPLATE pollen to germinate is most likely caused by the ectopic callose deposition between the plasma membrane and the intine layer.

TPLATE-GFP Accumulates at the Pollen Tube Exit Site upon Germination

Because pollen development requires TPLATE, we determined the localization of TPLATE-GFP in germinating pollen. The TPLATE-GFP protein was expressed in pollen from the Lat52 promoter, which is reported to have a pollen-specific expression pattern with only low transcript levels detectable in anther walls and petals (Ursin et al., 1989; Twell et al., 1990). Transcripts driven by the Lat52 promoter are first detected in spores undergoing pollen mitosis I and then increase substantially in mature pollen. GFP-tagged TPLATE protein expressed from Lat52 complemented the pollen phenotype of the *tplate* mutant. The ratio of wild-type versus mutant pollen was examined in *tplate* plants transformed with the *Lat52-TPLATE-GFP* construct. The plants were heterozygous for both T-DNAs, so complementation of the mutation caused by the insertion of the T-DNA in the *TPLATE* gene should result in a shift from a 1:1 ratio of wild-type versus mutant pollen to a 3:1 ratio. From 1325 pollen grains counted, 971 had a wild-type appearance and 354 were shriveled. This amounts statistically to the expected 3:1 ratio of two independently segregating insertions (χ^2 test for a 3:1 ratio yields 2.08, and χ^2 95% interval value is 3.84). The complementation was further substantiated by wild-type Columbia (Col-0) backcrosses. The *TPLATE* T-DNA insertion was transmitted to the wild-type plants via pollen that invariably also carried the *TPLATE-GFP* gene. Moreover, using PCR, we identified plants homozygous for the *TPLATE* T-DNA insertion in the backcrossed offspring (data not shown). We conclude that the GFP-tagged TPLATE protein, expressed by the Lat52 promoter, is functional in pollen.

In mature pollen, TPLATE-GFP, expressed from the Lat52 or the endogenous promoter, was cytoplasmic and granular (Figure 4A). Upon incubation of the pollen in germination medium, TPLATE-GFP accumulated at a distinct area at the cell periphery (Figure 4B). This region corresponds to the position where the pollen tube emerges (Figure 4C). Time-lapse recording further demonstrated that TPLATE-GFP is transported into the growing pollen tube (Figures 4C and 4D). The localization of TPLATE-GFP at the pollen tube exit site and at the tip of the pollen tube supports a role in the control of vesicle fusion.

Expression Analysis of *TPLATE*

The pollen-maturation phenotype of *TPLATE* T-DNA insertion plants and the subcellular localization of TPLATE-GFP in pollen suggest that the corresponding gene is activated in developing pollen. We analyzed the expression of TPLATE using a genomic fragment containing the open reading frame and 800 bp upstream of the start codon fused to the β-glucuronidase gene. β-Glucuronidase activity was detected in pollen grains and at the connectivum, where the anther is connected to the filament (see Supplemental Figure 1A online). A thorough study of whole-genome gene expression during different developmental stages of *Arabidopsis* pollen was performed previously (Honys and Twell, 2004). The *TPLATE* mRNA is expressed in uninucleate microspores and in bicellular and immature tricellular pollen, but it is low-abundant in dried, mature pollen grains. The same study

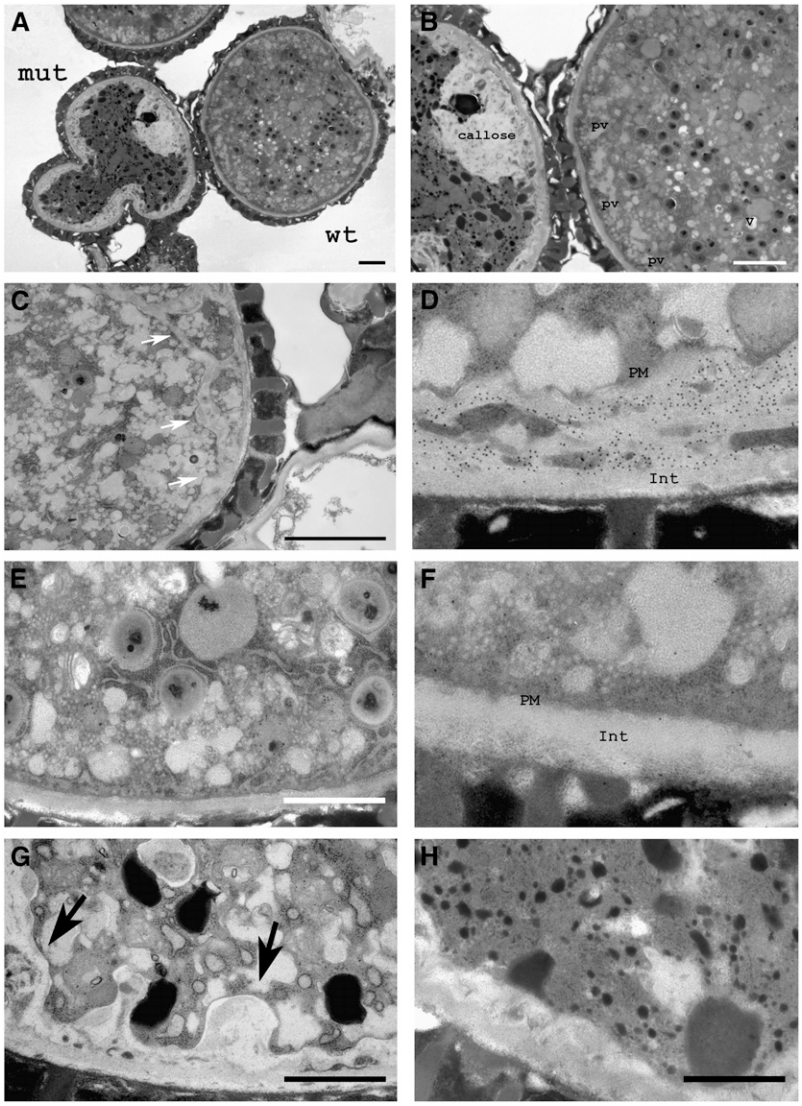

Figure 3. Electron Microscopy of *tplate* and Wild-Type Pollen.

(A) Overview of mutant and wild-type pollen grains.
(B) Close-up of **(A)**. Accumulation of callose is comparable to that seen in Figures 2G to 2I.
(C) Noncollapsed mutant pollen showing undulations of the plasma membrane (arrows). Bars = 2 μm for **(A)** to **(C)**.
(D) and **(F)** Immunoelectron microscopy sections of a mutant and a wild-type pollen grain using a callose-specific antibody. The mutant pollen shows gold labeling between the plasma membrane (PM) and the intine layer (Int), whereas hardly any label is present in nongerminated wild-type pollen. Bar = 1 μm.
(E), **(G)**, and **(H)** High-magnification images of wild-type and mutant pollen. Bars = 1 μm.
pv, peripheral band of vesicles; v, vacuole.

showed that TPLATE expression is not restricted to pollen (Honys and Twell, 2004) (see Supplemental Figure 1B online). *TPLATE* was originally identified through homology with a tobacco BY-2 cDNA-AFLP tag (BSTT43-4-330) with an M-phase–specific upregulation of expression (Breyne et al., 2002; Van Damme et al., 2004a). We determined TPLATE mRNA levels in *Arabidopsis* roots by whole-mount in situ hybridization. Transcript was present throughout the root tip meristem, although it was not distributed uniformly. The lowest level of expression was at the very tip end, and a stronger expression occurred near the elongation zone (see Supplemental Figures 1C to 1F online). The *TPLATE* expression pattern is in agreement with the results of previous digital in situ results (Birnbaum et al., 2003; www.arexdb.com) and does not match the expression pattern of cell cycle–controlled genes. Thus, *Arabidopsis TPLATE* is not likely to be cell cycle–controlled.

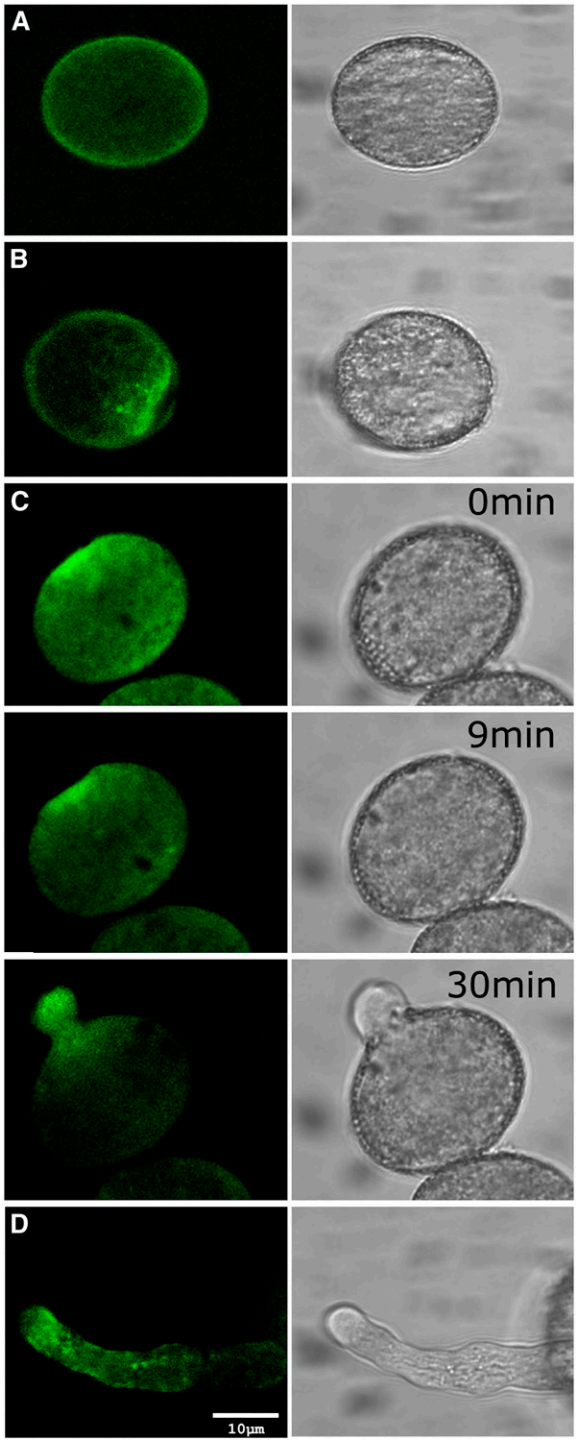

Figure 4. TPLATE-GFP Localization in Pollen.

(A) Confocal section of a nongerminating mature pollen grain expressing the TPLATE genomic construct showing diffuse labeling of TPLATE-GFP. The appearance of signal near the periphery is predominantly autofluorescent.

(B) Confocal section of TPLATE genomic-GFP accumulation at the future pollen tube exit site.

(C) Confocal sections of a Z-stack (10 sections, 7.35 μm) time-lapse series of germinating pollen grains showing accumulation of TPLATE-GFP at the future pollen tube exit site.

(D) Punctate localization of TPLATE genomic-GFP at the pollen tube tip.

TPLATE Is Required for Somatic Cytokinesis

The presence of *TPLATE* transcripts in somatic tissue suggests a role for TPLATE in somatic processes besides pollen development. *Arabidopsis* lines homozygous for the *TPLATE* T-DNA insertion that also carried the complementing *Lat52-TPLATE-GFP* did not show discernible growth or a morphological phenotype. Because of *Lat52-TPLATE-GFP* expression in seedlings, as shown by GFP fluorescence and protein gel blot analysis (see Supplemental Figure 2 online), any somatic phenotype is likely to be complemented in the homozygous *TPLATE* mutant lines by TPLATE-GFP expression.

Therefore, we decided to suppress TPLATE activity by post-transcriptional gene silencing. The *TPLATE* cDNA was expressed from the 35S promoter as a hairpin loop double-stranded RNA in *Arabidopsis*. Two independent hairpin constructs with different backbones yielded transgenic plants that displayed severe growth defects (Figures 5A and 5B). The expression of *TPLATE* in these plants was assessed by RT-PCR. Compared with wild-type plants, *TPLATE* expression was strongly reduced in the knockdown seedlings (Figure 5C). The mRNA level of a control gene, *eIF-4A-1*, was not affected, indicating that the growth defect in knockdown seedlings did not influence the expression of this household gene. The knockdown seedlings produced thickened cotyledons with an irregular surface and a reduced number of stomata (Figures 5A and 5B; data not shown). The hypocotyl was approximately twice as thick as wild-type hypocotyls, whereas the root diameter appeared normal (Figures 5I and 5J). Most plants were arrested at an early stage of development, although some of them produced a first set of leaves that did not fully expand and had a vitrified appearance (Figure 5B).

At 5 d after germination, mitotic cells were no longer detected by DAPI staining and growth was completely arrested (data not shown). A morphological analysis of PI-stained seedlings revealed the presence of interrupted cell walls and aberrant cell plates in epidermal cotyledon cells (Figure 5H) as well as in other cell types, but these were more difficult to analyze three-dimensionally.

Cellulose polymerization defects and weakening of the cell wall frequently go hand in hand with the stimulation of callose synthesis, which, besides its role in pollen development, normally occurs only in wounded tissue and in developing cell plates (Delmer and Amor, 1995; Nickle and Meinke, 1998; Gillmor et al., 2005). To test the presence of ectopic callose deposition in RNA interference (RNAi) *Arabidopsis* plants, transgenic material was stained with aniline blue and epifluorescence was imaged. Numerous depositions of ectopic callose were detected in cotyledons (Figure 5F) and in roots (Figure 5K). In wild-type plants, callose is detected in newly formed cell plates and in the junctions of stomatal guard cells (Figures 5G and 5L). In RNAi seedlings, callose depositions were most prominent in root tissue, in particular at the root tip (Figure 5K). The ectopic deposition of callose

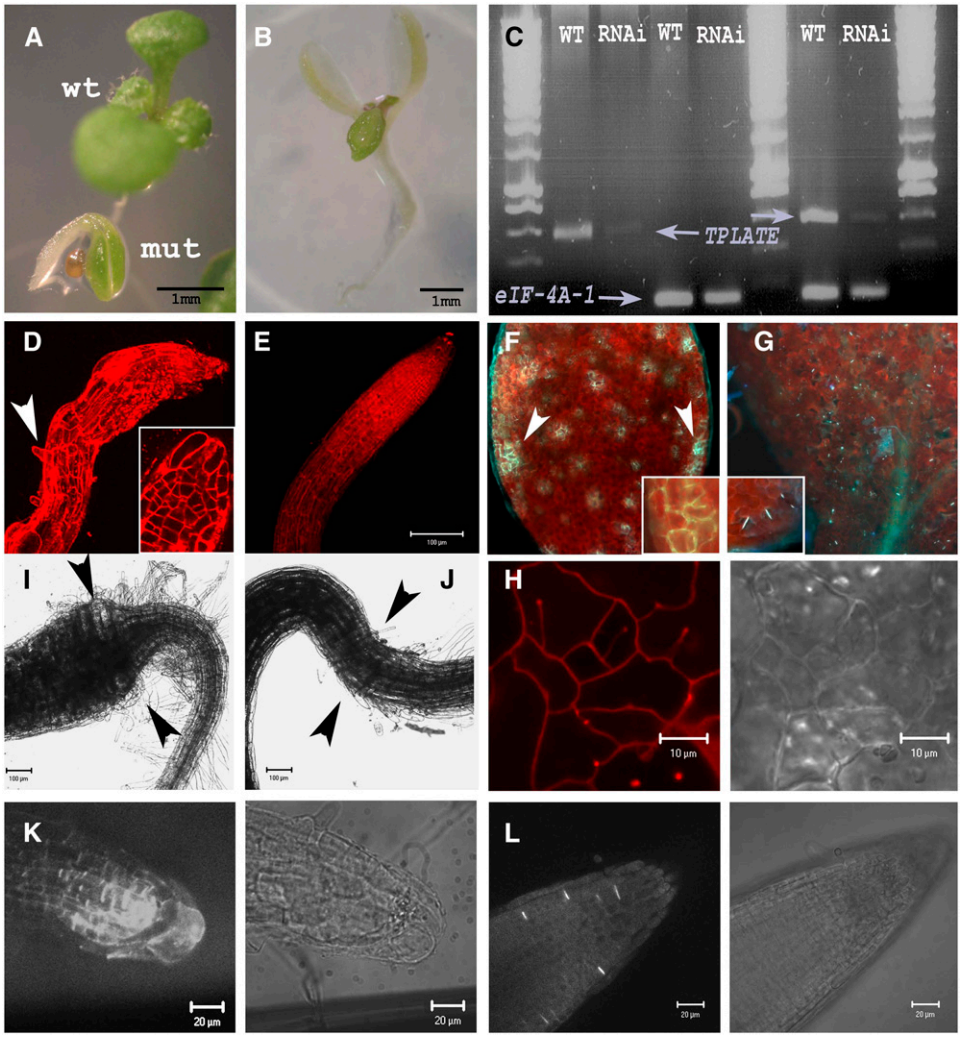

Figure 5. Silencing of the *TPLATE* Gene in *Arabidopsis* Seedlings.

(A) Overview of a *TPLATE* knockdown and a wild-type seedling germinated without selection.
(B) RNAi seedling forming a first pair of true leaves.
(C) Agarose gel showing reduced amplification of the *TPLATE* mRNA in the knockdown seedlings and amplification of *eIF-4A-1* as a control (left lanes) and amplification of both *TPLATE* and *eIF-4A-1* in a single reaction (right lanes).
(D) and **(E)** Confocal Z-stack projections taken at the same magnification of the root tip of an RNAi and a wild-type seedling stained with FM4-64. In RNAi mutants, root hairs emerge close to the tip (white arrowhead). The inset in **(D)** shows the aberrant morphology of the root tip in these RNAi seedlings.
(F) and **(G)** Epifluorescence images of an RNAi and a wild-type cotyledon showing ectopic callose deposition (yellow) visualized by aniline blue staining. The inset in **(F)** is a blow-up of an epidermal cell showing depositions of callose. Red signal is autofluorescent. In wild-type cotyledons, aniline blue labels only newly formed cell plates and stomatal guard cells (inset in **[G]**).
(H) Confocal section of PI-stained epidermal cells of *TPLATE* knockdown seedlings showing incomplete cell plates. Bars = 10 μm.
(I) and **(J)** Differential interference contrast images of the hypocotyl–root interphase (arrowheads) of an RNAi and a wild-type seedling.
(K) and **(L)** Confocal sections of an RNAi and a wild-type root stained with aniline blue. Images were made using the exact settings of laser power and pinhole diameter to visualize callose. Callose accumulates strongly in RNAi seedling roots compared with wild-type roots, where callose is present only in forming cell plates. Bars = 20 μm.

in silenced plants and cell cultures is indicative of a malfunctioning of cell wall formation or modification.

To investigate the growth inhibition and cytokinesis defects observed in *Arabidopsis* in more detail, *TPLATE* was silenced in BY-2 tobacco suspension cells using a homologous cDNA-AFLP fragment previously isolated from these cells (tag BSTT43-4-330) (Breyne et al., 2002). The *TPLATE* RNAi calli grew significantly slower than calli transformed with unrelated constructs (data not shown). In >20 independent transformation events that were analyzed, ~10% of the BY-2 cells had misplaced cell walls

(deviations ≥ 90°) or produced cell walls with severe deformations. Examples of aberrant cross walls are presented in Supplemental Figure 3 online.

In addition, we observed that cell plates did not always fuse to the mother wall and produced fuzzy extreme ends. Figure 6 shows a time-lapse recording of a *TPLATE* RNAi BY-2 cell stained with FM4-64 that failed to anchor its newly formed cell plate.

The plate is initially made and expands until it reaches the cortex (Figure 6, image after 62 min) but subsequently fails to insert, even when the cell is followed for >90 min after contact of the cell plate with the cortex. The cell in Figure 6 also shows ectopic growth, which is commonly observed in *TPLATE* RNAi BY-2 cell lines and may be caused by mistargeting of cell wall–modifying factors, as a result of the reduced activity of TPLATE. The RNAi effects in *Arabidopsis* and BY-2 cells confirm that TPLATE is required for somatic cytokinesis and anchoring of the cell plate with the mother wall.

Root and Hypocotyl Tissues from TPLATE RNAi Plants Are Severely Disorganized

Root morphology was determined for several RNAi plants (Figures 5D and 5E). The meristematic tissue contained differentiated cells, and root hairs emerged close to the tip (Figure 5D, arrowhead). Figure 7 shows toluidine blue–stained transverse sections of wild-type and *TPLATE* RNAi root–hypocotyl and hypocotyl sections.

Some radial patterning can be observed in the RNAi seedlings, with smaller cells in the vascular bundle surrounded by larger cells of the endodermis, cortex, and epidermis. However, the vascular cylinder in the RNAi plants is severely disorganized, and cortical layers cannot be distinguished clearly (Figure 7B). In all transverse *TPLATE* RNAi hypocotyl sections examined, the cyan blue coloration typical for toluidine blue–stained wild-type xylem vessel cells (arrows in Figure 7A) was absent, indicating that these seedlings did not produce differentiated xylem elements. Figures 7C and 7D show sections at identical magnifications through the hypocotyl of a wild-type and an RNAi seedling. The central cylinder and cortical layers are present in the RNAi seedling section, although it is difficult to discriminate between the different layers. Incomplete and malformed cell walls are observed in the cortex of RNAi hypocotyls (Figures 7D, inset, and 7E). In addition, there are extra random divisions, predominantly in the vascular tissue (Figure 7D), leading to an increase in hypocotyl diameter. The central cylinder cells are not converted to vascular tissue, as in the wild type. Instead, they differentiate to starch-containing cells, as revealed by Lugol staining (Figure 7F, inset). Starch accumulation inside the vascular bundle was never observed in wild-type hypocotyl sections (data not shown). Therefore, reducing *TPLATE* expression leads to altered differentiation and extra rounds of cell division, predominantly in the vascular bundle.

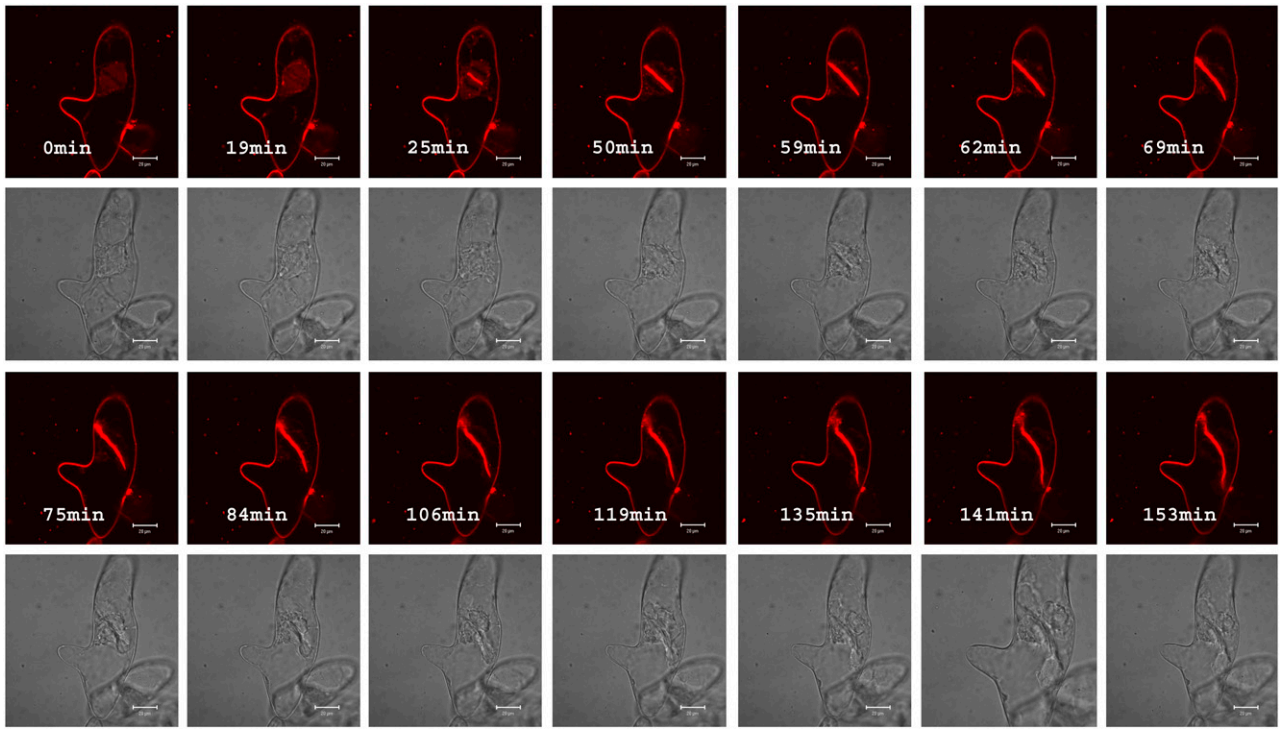

Figure 6. RNAi Effects in BY-2 Time Lapse.

Time-lapse recording of a BY-2 cell transformed with the pH7GWIWG(II) vector containing the tobacco *TPLATE* tag BSTT43-4-330, showing a dividing cell stained with FM4-64 that fails to insert the newly formed cell plate. Bars = 20 μm.

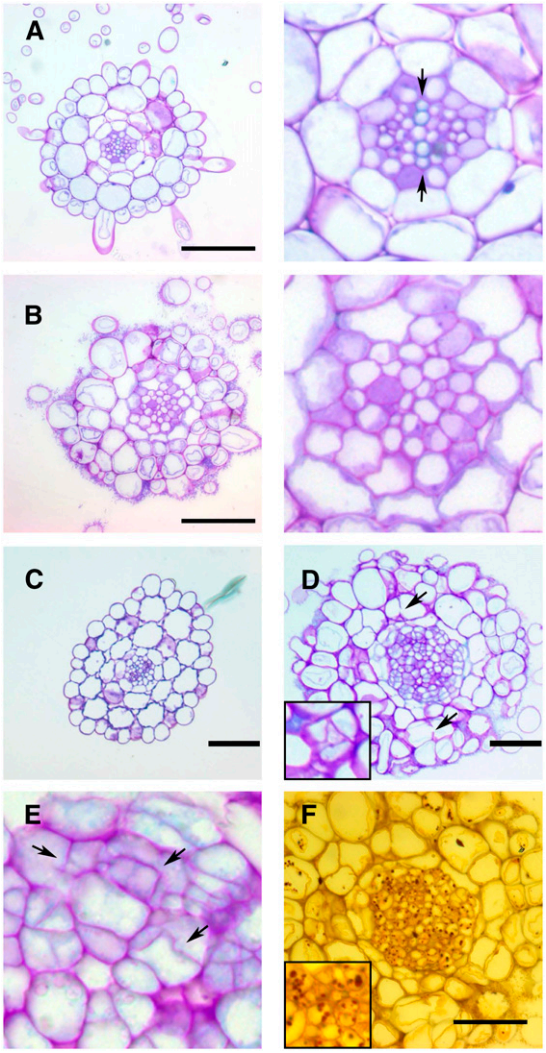

Figure 7. Transverse Hypocotyl Sections of RNAi Seedlings Reveal Aberrant Cell Fates of Vascular Cells.

(A) Toluidine blue–stained section of a wild-type root–hypocotyl junction and blow-up of the vascular system. Xylem cells are stained light blue and indicated with arrows.
(B) Toluidine blue–stained section of an RNAi root–hypocotyl junction and blow-up of the vascular system. Small cells in the vascular cylinder are formed, but based on the absence of the blue coloration representative of xylem cells, differentiation and patterning are lost.
(C) Toluidine blue–stained wild-type hypocotyl section.
(D) Toluidine blue–stained RNAi hypocotyl section taken at the same magnification. Arrows indicate incomplete cell plates. The inset shows a blow-up of a cell with aberrant division plane orientation.
(E) Blow-up of the vascular system of an RNAi hypocotyl section. Arrows indicate misguided cell plates.
(F) RNAi hypocotyl section from Figure 6D and blow-up (inset) stained with Lugol. Vascular cells accumulate starch granules.
Bars = 100 μm.

TPLATE Connects the Cell Plate with the Mother Wall

To investigate the subcellular localization of TPLATE in a tissue context, we analyzed *Arabidopsis* plants carrying an N- or C-terminally fused TPLATE construct with GFP behind the 35S promoter. *Arabidopsis* leaves were imaged with the confocal microscope within the first 24 to 36 h after germination, when numerous leaf epidermal cells and root meristematic cells divide (Figure 8).

GFP fluorescence was observed mainly in the cytoplasm of nondividing cells with both constructs. During cytokinesis, N- and C-terminally fused TPLATE concentrated at the developing cell plate (Figure 8, asterisks). The fusion proteins associated with the newly formed cell plate at an early stage of phragmoplast development (Figures 8C, 8D, and 8I). Upon contact of the cell plate with the mother wall, GFP fluorescence accumulated at the contact site, spreading over a region of ~5 μm surrounding the insertion site (Figures 8E and 8F, yellow arrowheads, and inset in 8F).

The accumulation of TPLATE fused to GFP at the division zone, together with the observation that in RNAi lines cell plates failed to or did not correctly connect to the mother wall, suggest that TPLATE plays a role in anchoring the cell plate to the mother wall.

DISCUSSION

TPLATE is a plant-specific protein that is essential for the formation of viable pollen grains and for the final steps of cytokinesis in somatic cells. This conclusion is supported by the male sterility of a *tplate* T-DNA insertion mutant, by the observation that TPLATE-GFP temporally accumulated at a narrow zone along the plasma membrane where the cell plate makes contact with the mother wall, and by the observation that downregulation of *TPLATE* results in anchoring defects. Nonconventional types of cytokinesis, such as male and female gametophyte development, were apparently unaffected in the *tplate* mutant, suggesting that the cortical localization of TPLATE-GFP is driven by a PPB-dependent process. In agreement with this notion, the peripheral region occupied by TPLATE-GFP corresponds to the division zone formerly marked by the PPB during the early steps of mitosis. The accumulation of TPLATE when the cell plate is in close proximity to the mother wall suggests that TPLATE contributes to cell plate formation and positioning during the final steps of cytokinesis.

Pollen germination and somatic cytokinesis involve substantial vesicle transport and fusion and, therefore, not surprisingly, become rate-limiting when one of the components is reduced or missing. *Arabidopsis* mutants with defective vesicle transport machinery usually display pleiotropic cellular phenotypes that culminate in a general growth disorder (Kang et al., 2001; Sanderfoot et al., 2001; Geelen et al., 2002). However, vesicle trafficking and fusion can also be dependent on a highly selective component that is restricted to a single process. The prime example for such selectivity is the KNOLLE syntaxin specifically involved in somatic cytokinesis (Müller et al., 2003).

Here, we describe a putative membrane traffic protein that is required in two seemingly unrelated cellular processes: pollen germination and somatic cytokinesis. Both phenomena necessitate the modification of the cell wall at a specific site where new wall material joins the existing wall. The targeting of GFP-tagged

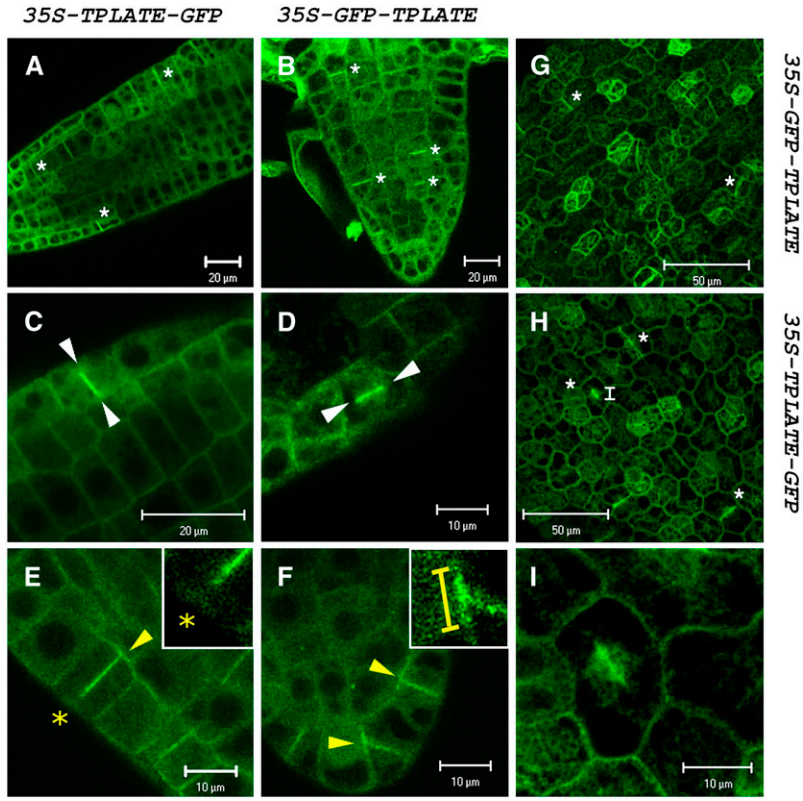

Figure 8. Localization of TPLATE-GFP and GFP-TPLATE in *Arabidopsis* Root and Leaf Epidermal Cells.

(A) and **(B)** Overview of TPLATE-GFP and GFP-TPLATE in *Arabidopsis* root cells. The fusion protein accumulates in the midline of dividing cells (asterisks).

(C) and **(D)** Close-up of midline targeting of the fusion protein in a young phragmoplast of *Arabidopsis* root cells (between white arrowheads).

(E) and **(F)** Close-up of the fusion protein accumulating in the midline of the phragmoplast and the division zone (yellow arrowheads). The inset in **(E)** shows that plasma membrane labeling of TPLATE-GFP is absent before plate insertion (asterisk) into the mother wall. The inset in **(F)** shows a blow-up of the accumulation of GFP-TPLATE (yellow bar) at the division zone upon plate insertion.

(G) and **(H)** Localization of GFP-TPLATE and TPLATE-GFP in leaf epidermal cells of *Arabidopsis* at 24 to 36 h after germination. Asterisks indicate accumulation of the fusion protein in the midline of dividing cells.

(I) Magnification of a dividing epidermal cell (indicated with I in **[H]**) showing midline targeting of TPLATE-GFP.

TPLATE during cytokinesis and pollen germination to the division site and the pollen tube exit site, respectively, suggests that TPLATE contributes to these cell wall modifications (see Supplemental Figure 4 online).

The TPLATE Protein Shows Similarity to the COPI Proteins

Adaptor protein complexes are involved in the formation of clathrin-coated vesicles, occurring in endocytic and recycling pathways between the plasma membrane and the lysosomes or the *trans*-Golgi network (Kirchhausen et al., 1997; McMahon and Mills, 2004). The TPLATE protein shows similarity to the adaptin_N domain of COP proteins; in addition, TPLATE proteins contain a 14–amino acid motif that is highly conserved in all β-COP proteins. We designated this motif the β-COP–specific element.

Cell plate formation relies on massive vesicle transport along the phragmoplast microtubules and involves homotypic fusion of these vesicles to produce a solid cell plate at the center of the cytokinetic cell (Jürgens, 2005a). Similar to TPLATE, COPI proteins accumulate at the phragmoplast midline, where the cell plate is formed (Couchy et al., 2003; Vanstraelen et al., 2006). To date, it is not yet clear how important these coat proteins are for the formation of the cell plate.

TPLATE-GFP Concentrates at Sites Where Vesicle Fusion Takes Place

GFP-tagged TPLATE concentrates between the separated chromatin when the phragmoplast emerges at the cell center. The GFP signal follows the laterally expanding cell plate up to the moment of contact with the mother wall (Van Damme et al., 2004a). Remarkably, TPLATE also concentrates at the cortical division zone when the cell plate approaches the mother wall (Figures 8E and 8F; see Supplemental Figure 4 online). The protein accumulates along a stretch ~5 μm wide at the final insertion site.

At the cell plate, vesicle fusion drives cell plate formation and allows the plate to expand in a centrifugal manner. The vesicle fusion process is mediated by an essential, cytokinesis-specific syntaxin (KNOLLE), a SNARE member that cooperates with other membrane proteins to form a vesicle fusion complex (Lauber et al., 1997; Müller et al., 2003; Jürgens, 2005a). Because cell plates are made de novo, at first there is no target membrane and vesicle fusion must primarily be homotypic. Plasma membrane and cell plate composition are not identical; thus, attachment of the cell plate to the mother wall probably depends on a heterotypic fusion process that may require a different set of SNARE proteins (Jürgens, 2005a; Vanstraelen et al., 2006). *knolle* mutants are impeded in making correct cell plates but frequently produce small cell wall stubs associated with the mother wall. These stubs may result from continued vesicle deposition at the insertion site in an attempt to make contact with a cell plate that in the end does not form. The formation of these stubs in the *knolle* mutant indicates that the KNOLLE complex is not essential for the connection of the cell plate with the mother wall. A cell plate was still formed in *TPLATE* knockdown *Arabidopsis* cells and BY-2 cell lines. However, these plates were not rigid as in wild-type cells, and they did not always connect properly to the mother wall. Possibly, cell plates did not attach correctly to the mother wall and therefore did not mature as in wild-type cells, leading to crooked shapes, in agreement with previous reports (Palevitz, 1980; Mineyuki and Gunning, 1990).

In germinating pollen, TPLATE-GFP accumulates in a punctate manner at the site of pollen tube exit and later travels toward the tip of the growing pollen tube (Figure 4; see Supplemental Figure 4 online). Pollen tube growth relies heavily on extensive vesicle transport to the tube tip and subsequent fusion of vesicles to the plasma membrane to allow expansion and the secretion of cell wall components (Hepler et al., 2001). The secretion of vesicles is a heterotypic fusion process whereby specific target SNAREs or syntaxins at the plasma membrane are needed (Carter et al., 2004). The involvement of TPLATE in pollen tube emergence and growth distinguishes it from KNOLLE, because the *knolle* mutants do not produce defective pollen grains. The function of KNOLLE is restricted to homotypic vesicle fusion processes that may not be primordial for pollen tube formation (Müller et al., 2003). TPLATE, on the other hand, might be important in facilitating heterotypic vesicle fusion.

Ectopic Callose Deposition in *tplate* Mutants

Mature *tplate* mutant pollen contained extensive depositions of callose laid as irregular formations against the intine cell wall layer. Intine and exine appeared morphologically identical to those of wild-type pollen, indicating that callose deposition did not interfere with cell wall formation and likely occurred after wall formation had been completed. Based on appearance in electron micrographic recordings, differences in vesicle composition between wild-type and mutant pollen were observed. The most affected pollen contained fewer vesicles, and the diversity based on electron density was altered. Whether these differences in vesicle composition are the cause of ectopic callose formation remains to be determined. Relatively little is known about the composition and dynamics of vesicles in pollen. Most information comes from electron microscopic observations, by which it was determined that cell wall precursor–containing vesicles localize predominantly at the peripheral border near the intine layer (Van Aelst et al., 1993). The precursor vesicles accumulate in large amounts at the periphery to support the very fast mode of germination observed for *Arabidopsis* pollen (Heslop-Harrison, 1987; Pickert, 1988). Because TPLATE-GFP is concentrated at the cell periphery during pollen exit site establishment and at the pollen tube tip, it is possible that TPLATE is involved in vesicle targeting and fusion with the plasma membrane.

The TPLATE pollen morphology strongly resembles that of *adl1C* mutant pollen (Kang et al., 2003a; ADL1C was renamed DRP1C by Hong et al. [2003a]). The *adl1C* mutation specifically affects male gametogenesis and leads to the production of shriveled pollen that fails to germinate. Remarkably, the *adl1C* and *tplate* mutations are fully penetrant, which is not so for several other male-sterile mutants (Kang et al., 2003a; this work). Similar to *tplate* pollen, *adl1C* pollen grains contain cell wall depositions close to the intine layer, the plasma membrane is heavily undulated, and vesicle composition is changed. The desiccation intolerance and shriveled appearance of both *adl1C* and *tplate* pollen is in agreement with a critical requirement of an intact intine wall for pollen germination and survival (Grini et al., 1999; Fei and Sawhney, 2001). DRP1C is a member of the dynamin-like protein family, which in animal cells function in both clathrin-mediated and non-clathrin-mediated endocytic processes (Praefcke and McMahon, 2004).

Plant dynamins are subdivided into six families based on functional motifs (Hong et al., 2003a). Members of the *Arabidopsis* DRP1 family, which is most related to soybean (*Glycine max*) PHRAGMOPLASTIN, mediate membrane tubule formation and function in vesicle trafficking from Golgi to the cell plate (Gu and Verma, 1996; Hong et al., 2003b; Kang et al., 2003a, 2003b). The striking similarity between the pollen phenotypes conferred by *tplate* and *adl1C* together with the cell plate localization of both proteins during cytokinesis reinforce the idea that TPLATE functions in the regulation of vesicular traffic. Callose depositions were also observed in dividing cells in cotyledons and in roots in *TPLATE* RNAi seedlings, where vesicle composition is likely very different from that in pollen.

Ectopic callose is often regarded as an indication of compromised cell wall integrity and occurs in response to stress situations (Gillmor et al., 2005). Defective cellulose deposition triggered by cellulose biosynthesis inhibitors, such as dichlorobenzonitrile or isoxaben (Desprez et al., 2002), or attributable to a cellulose deficiency mutation, as in *cyt1* embryos (Nickle and Meinke, 1998; Lukowitz et al., 2001), leads to the accumulation of ectopic callose. Ectopic callose has also been seen to accumulate in embryos carrying a double mutation in the dynamins *adl1A* and *adl1E* (Kang et al., 2003b). The overexpression of PHRAGMOPLASTIN or a GTPase-defective form of PHRAGMOPLASTIN caused a persistence of callose in fully completed cell plates. Here, the mispositioning of cell plates during megaspore development is believed to retard or obstruct cell plate maturation (Geisler-Lee et al., 2002; Hong et al., 2003b). Cell plates that connect with the mother wall at unprepared sites seem not to flatten (Palevitz, 1980), possibly because the division zone contains some essential cell wall maturation factors (Mineyuki and

Gunning, 1990). The embryonal cytokinesis defects in *knolle* and *keule* mutants do not display the accumulation of ectopic callose (Nickle and Meinke, 1998). Incomplete cell wall formation in plants without callose accumulation is phenocopied by *caffeine*, an inhibitor of Ca^{2+}-controlled vesicle-trafficking processes (Hepler and Bonsignore, 1990) that resembles the *cyd* mutant of pea (*Pisum sativum*) (Liu et al., 1995). It is not the intrinsic strength of the cell wall in these cytokinesis mutants that is affected; rather, walls are missing or incomplete. The observations that cell plates can form and that callose persists in TPLATE RNAi seedlings and BY-2 cells suggest that TPLATE is more likely to be involved in cell wall modification and maturation than in the primary steps of plate formation.

TPLATE Is Required for Cell Plate Positioning and Cell Differentiation

Reduced expression of the *TPLATE* gene by RNAi resulted in the formation of distorted and sometimes incomplete cell walls. *TPLATE* is a singleton in *Arabidopsis* with low overall nucleotide similarity to genomic sequences, reducing the chance that other genes are silenced too. Knockdown plants sometimes produced a first pair of leaves. Regardless of the development of leaves, all plants died within a few weeks after germination. It is possible that the extended life span compared with other cytokinesis mutants is attributable to the low activity of the 35S promoter during embryogenesis, allowing growth beyond the embryonic heart stage (Odell et al., 1994; Völker et al., 2001).

TPLATE RNAi seedlings had a radially expanded hypocotyl similar to that of the cellulose-deficient mutants *kor1-2/rsw2*, *rsw1/cesA1*, *kob1*, and *procuste1* (Arioli et al., 1998; Nicol et al., 1998; Fagard et al., 2000; Peng et al., 2000; Lane et al., 2001; Williamson et al., 2001; Beeckman et al., 2002; Pagant et al., 2002). With the exception of *kor1-2*, these mutants have a thickened hypocotyl without severe impact on tissue organization or development of the vascular tissue. The *kor1-2* mutant lacks distinct cell files in roots, hypocotyls, and cotyledons, shows impaired vascular tissue development, and cell divisions occur randomly (Zuo et al., 2000). Similar defects in cell file organization and random cell divisions are found in the *TPLATE* RNAi seedlings. At the cellular level, *kor1-2* mutants show misplaced and distorted cell plates that often terminate before reaching the mother wall (Zuo et al., 2000). *TPLATE* RNAi seedlings also produced cells with interrupted and misplaced cell walls. The imperfect separation of dividing cells may account for miscommunication among neighboring cells whereby cell differentiation is disturbed and the tissues become improperly organized (Lukowitz et al., 1996). Perhaps such miscommunication provokes the formation of the starch-containing cells seen in the *TPLATE* RNAi hypocotyl sections. The occurrence of inadvertent cell divisions at the central cylinder is probably not responsible for the altered differentiation in the hypocotyl of *TPLATE* RNAi seedlings, as additional vascular divisions also occur in the mutant *fass* without a loss of correct vascular differentiation (Torrez-Ruiz and Jürgens, 1994). Extra cell divisions in the central cylinder have also been reported for the cellulose-deficient *rsw2-1* mutant of *Arabidopsis*, which is allelic to *kor1-2* (Lane et al., 2001). *KOR1* encodes a membrane-anchored endoglucanase (KORRIGAN) that is assumed to function in cell wall modification and maturation. TPLATE may contribute to cell wall maturation too, as cell plates and cell walls appear less strong in RNAi BY-2 cells.

Although several lines of evidence support a direct role for TPLATE in cell plate maturation, it is possible that incomplete cell walls and ectopic callose deposition are secondary effects of *TPLATE* silencing. Nevertheless, the subcellular distribution of TPLATE holds the promise that its primary function is to ascertain correct plasma membrane targeting (see Supplemental Figure 4 online). In the absence of TPLATE, specialized vesicles are no longer correctly formed or, more likely, they are inapt for site-directed targeting to the plasma membrane. The fact that the TPLATE mutation was pronounced in pollen and did not have a discernible effect on female gametophyte fertility may reflect a differential requirement for plasma membrane targeting between these cell types. TPLATE is clearly also essential for normal somatic development. Silencing of TPLATE has pleiotropic effects, including changes in cell division and cellular differentiation. Together, our findings have led to an unexpected link between the vesicle–plasma membrane interphase in pollen and cell plate maturation and attachment during cytokinesis.

METHODS

T-DNA Insertion Mutant Analysis

Arabidopsis thaliana SALK_0030086 was obtained from the SALK collection (Alonso et al., 2003). Genomic DNA was extracted, and PCR to identify the insertion was done using the LP and RP primers (5′-CCCTTGGCAATTTTCCTCGAA-3′ and 5′-TGCAAAGTGACCCTTCCATCA-3′) that were recommended by the SIGNaL iSect Tool of The Arabidopsis Information Resource database (www.Arabidopsis.org) in combination with the T-DNA–specific LBa1 primer (5′-TGGTTCACGTAGTGGGCCATCG-3′).

Thin Sections

Whole-mount anther and seedling sections were prepared according to De Smet et al. (2004). Thin sections (5 μm) were made using a Rotation Microtome 2040 (Leica Microsystems) using glass knives (Leica Microsystems) for transverse sections and Superlap knives (Adamas Instrumenten) for longitudinal anther sections. Transverse sections of roots and hypocotyls were stained with 0.05% toluidine blue O (Sigma-Aldrich) in 0.1 M $NaPO_4$ buffer, pH 7.0, and 1% Lugol solution (Merck) for starch staining.

Pollen Analysis

Pollen morphology was analyzed using light microscopy (DMLB; Leica). The pollen was stained with Alexander stain (Alexander, 1969), and mutant versus wild-type pollen grains were counted. Germination of pollen grains in vitro was performed as described by Chen and McCormick (1996). Anthers were stained with DAPI staining solution (0.1% Nonidet P-40, 10% DMSO, 50 mM PIPES, 5 mM EGTA, and 1 μL of DAPI; 1 mg/mL).

PI (Sigma-Aldrich) staining of thin anther sections was done by adding 30 μM PI to the slides and washing them after 5 min of incubation. Aniline blue (0.5% in water; Sigma-Aldrich) and calcofluor white (1% in water, fluorescent brightener 28; Sigma-Aldrich) were added simultaneously to the thin anther sections, and slides were washed after 5 min of incubation.

Fluorescent Protein Fusion Constructs and Transformation

The construct to drive *TPLATE-GFP* expression under the control of the Lat52 promoter was created using the multisite Gateway system (Invitrogen) (Karimi et al., 2005). *pDONRP4-P1R-Lat52*, *pDONR207-TPLATE*, and *pDONRP2R-P3-EGFP* were used to clone the Lat52 promoter, the *TPLATE*, and the *EGFP* open reading frames in pH7m34GW. pLAT52-7 (Bate et al., 1996) was kindly provided by David Twell and was used for PCR of the Lat52 promoter and cloning in pDONRP4-P1R using the following primer pair: 5′-GGGGACAACTTTGTATAGAAAAGTTGGTCGACATACTCGACTCAGAAGGTAT-3′ and 5′-GGGGACTGCTTTTTTGTACAAACTTGGTGTCTTGTTTTGATTATA-3′.

The genomic fragment of the *TPLATE* gene (5.1 kb) was amplified by PCR using Gateway adapted primers (FW, 5′-GGGGACAAGTTTGTACAAAAAAGCAGGCTTTTATTGTTCCTCACAGTCATGATATCGC-3′; REV, 5′-GGGGACCACTTTGTACAAGAAAGCTGGGTTGTTAACTTTGGTATATTTTCTATCTTTGCAC-3′) and cloned into an adapted version of the pK7GWFS7 plasmid to allow in-frame translational fusion between the TPLATE protein, β-glucuronidase, and EGFP. Expression of the *TPLATE* messenger was analyzed by β-glucuronidase expression, and the fusion protein was localized by GFP fluorescence using confocal microscopy.

35S-GFP fusion constructs and transformation of tobacco (*Nicotiana tabacum*) BY-2 cells have been described by Van Damme et al. (2004a, 2004b). Cotransformations in BY-2 cells were obtained by consecutive transformations. *Arabidopsis* ecotype Col-0 plants were transformed by *Agrobacterium tumefaciens*–mediated transfection using the floral dip method (Clough and Bent, 1998).

Microscopy and Drug Treatments

Image acquisition was as described by Van Damme et al. (2004b). PI staining and differential interference contrast images of anther sections were obtained with a 100M confocal microscope with software package LSM510 version 3.2 (Zeiss) equipped with a 63× water-corrected objective (numerical aperture = 1.2) using the settings for RFP excitation and emission (excitation = 543 nm; emission = 560 nm cutoff). Aniline blue, calcofluor, and DAPI staining were imaged using an Axiovert 135M fluorescence microscope equipped with a 63× water-corrected objective (numerical aperture = 1.2) with emission and excitation filters (excitation = 395 nm; emission = 420 nm long pass), and images were taken with an Axiocam camera and Axiovision software version 3.1 (Zeiss). Thin root sections on slides were analyzed by a light microscope (DMLB; Leica) equipped with a 40× objective, and images were taken with an Axiocam camera and Axiovision software version 3.1 (Zeiss).

Arabidopsis seedlings were imaged between slide and cover glass. Aniline blue (0.5% in water) and FM4-64 (50 μM; Invitrogen) were added to whole *Arabidopsis* seedlings and imaged after a 5-min incubation. BY-2 cells were applied to a chambered cover glass system (Lab-Tek). Cells were immobilized in a thin layer of 200 μL of BY-2 medium containing vitamins and 0.8% low-melting-point agar (Invitrogen). FM4-64 (50 μM) and PI (30 μM) were added to 1 mL of liquid BY-2 medium with vitamins, and the drug concentration was adjusted to a final volume of 1.2 mL before addition to the samples. Stock solutions of FM4-64 (5 mM) and PI (1.5 mM) were prepared in nanopure water. Fluorescence intensity graphs were made using the profile program of the LSM software (Zeiss). Pollen expressing *Lat52-TPLATE-GFP* was analyzed by confocal microscopy on slides coated with germination medium.

Complementation of the TPLATE Mutation

Plants heterozygous for the T-DNA insertion in *TPLATE* (SALK_0030086) were transformed with the *Lat52-TPLATE-EGFP* construct. Seeds were selected on K1 medium (4.308 g/L Murashige and Skoog basal salt mixture; Duchefa), 10 g/L sucrose (Acros Organics), 100 mg/L *myo*-inositol (Sigma-Aldrich), 0.5 g/L MES (Duchefa), pH 5.7, with KOH, and 8 g/L plant tissue culture agar (International Diagnostics Group) with 15 μg/mL hygromycin B (Duchefa). The presence of the T-DNA was identified by PCR using the RP and LBal primers. Pollen of T-DNA– and *Lat52-TPLATE-GFP*–positive plants was used to pollinate Col-0 plants, and transmission of the T-DNA insertion via the parental route was checked by PCR on the offspring plants.

Electron Microscopy Analysis

For scanning electron microscopy, air-dried pollen was tapped on stubs, sputter-coated with gold, and examined with a scanning microscope (JEOL) under an acceleration voltage of 10 kV. For transmission electron microscopy, tissue samples were immersed in a fixative solution of 2% paraformaldehyde and 2.5% glutaraldehyde and postfixed in 1% OsO_4 with 1.5% $K_3Fe(CN)_6$ in 0.1 M Na-cacodylate buffer, pH 7.2. Samples were dehydrated through a graded ethanol series, including a bulk staining with 2% uranyl acetate at the 50% ethanol step, followed by embedding in Spurr's resin. Ultrathin sections, made on an Ultracut E microtome (Leica Microsystems), were poststained in an ultrastainer (Leica) with uranyl acetate and lead citrate. Samples were viewed with a 1010 transmission electron microscope (JEOL).

For immunoelectron microscopy analysis, root tips of 4-d-old *Arabidopsis* seedlings (Col-0 ecotype) were excised, immersed in dextran (20%), and frozen immediately in a high-pressure freezer (EM Pact; Leica Microsystems). Freeze substitution was performed in a Leica EM AFS. Over a period of 4 d, root tips were substituted in dry acetone + 0.1% OsO_4. Samples were infiltrated at 4°C stepwise in Spurr's resin and embedded in molds. The polymerization was performed at 70°C for 16 h. Ultrathin sections of gold interference color were cut using an ultramicrotome (ultracut E; Reichert-Jung) and collected on formvar copper slot grids. All steps of immunolabeling were performed in a humid chamber at room temperature. Samples were blocked in blocking solution (5% BSA and 1% fish skin gelatin in PBS) for 15 min followed by a wash step for 5 min (1% BSA in PBS). Incubation in a dilution (1% BSA in PBS) of primary antibodies (anti-callose 1:100; Biosupplies Australia) for 60 min was followed by washing four times for 5 min each (0.1% BSA in PBS). The grids were incubated with 10-nm Protein A Gold (Cell Biology, Utrecht University) and washed twice for 5 min each (0.1% BSA in PBS, PBS, and double distilled water). Sections were poststained in a LKB ultrastainer for 30 min in uranyl acetate at 40°C and for 5 min in lead stain at 20°C. Control experiments consisted of treating sections with 10-nm Protein A Gold alone. Grids were viewed with a JEOL 1010 transmission electron microscope operating system at 80 kV.

RNAi Experiments

The *TPLATE* coding sequence was cloned into the pK7GWIWG(II) or pH7GWIWG(II) vector (Karimi et al., 2002) to produce double-stranded RNA, and *Arabidopsis* Col-0 plants were transformed. Transformed seeds were selected on K1 medium with 25 μg/mL kanamycin A (Duchefa) or 15 μg/mL hygromycin B (Duchefa). BY-2 cells were transformed with the vector pH7GWIWG(II) containing the BSTT43-4-330 tobacco tag (Breyne et al., 2002), and calli were selected on hygromycin B (30 μg/mL; Duchefa).

RT-PCR

Arabidopsis seedlings were ground, and the RNA was extracted using the RNeasy kit (Qiagen). The RNA concentration was adjusted, and 1 μg of total RNA was used for cDNA amplification (Superscript RNA polymerase III; Invitrogen). PCR was performed using the following primer pairs:

for *TPLATE* amplification, 5′-CGTGTGGATATACGGGTTGGATT-3′ and 5′-CGCCAAAGATCATCATACCC-3′ to amplify a 600-bp band; and for *eIF-4A-1* (At3g13920), 5′-ACGGAGACATGGACCAGAAC-3′ and 5′-GCTGAGTTGGGAGATCGAAG-3′ to amplify a 150-bp band.

Whole-Mount in Situ Hybridization

Probe synthesis and whole-mount in situ hybridization were performed as described by Friml et al. (2003) on *Arabidopsis* Col-0 seedlings and *Arabidopsis* 35S-TPLATE-GFP–expressing seedlings. The sense and antisense probe mix consisted of a mixture of four separate probes (250, 400, 490, and 600 bp) directed against different positions of the *TPLATE* messenger.

Accession Number

The Arabidopsis Genome Initiative locus identifier for TPLATE is At3g01780.

Supplemental Data

The following materials are available in the online version of this article.

Supplemental Figure 1. Expression Data of TPLATE.

Supplemental Figure 2. Ectopic Expression of *Lat52-TPLATE-GFP*.

Supplemental Figure 3. RNAi Effects in BY-2 Cells.

Supplemental Figure 4. Model of TPLATE Function in Pollen Germination and in Somatic Cytokinesis.

ACKNOWLEDGMENTS

We thank Rita Van Den Driesche for scanning electron microscopy, Hugh Dickinson and Heather Owen for help with the pollen morphology phenotype, David Twell for the Lat52 promoter, Toshiyuki Nagata and Yasunori Machida for suggesting the callose staining, and Martine De Cock for layout. S.C. is indebted to the Institute for the Promotion of Innovation by Science and Technology in Flanders for a predoctoral fellowship. D.V.D. is a Postdoctoral Fellow and D.G. was a Postdoctoral Researcher of the Research Foundation-Flanders.

Received January 6, 2006; revised October 5, 2006; accepted November 10, 2006; published December 22, 2006.

REFERENCES

Alexander, M.P. (1969). Differential staining of aborted and non-aborted pollen. Stain Technol. **44,** 117–122.

Alonso, J.M., et al. (2003). Genome-wide insertional mutagenesis of *Arabidopsis thaliana.* Science **301,** 653–657.

Arioli, T., et al. (1998). Molecular analysis of cellulose biosynthesis in *Arabidopsis.* Science **279,** 717–720.

Bate, N., Spurr, C., Foster, G.D., and Twell, D. (1996). Maturation-specific translational enhancement mediated by the 5′-UTR of a late pollen transcript. Plant J. **10,** 613–623.

Beeckman, T., Przemeck, G.K.H., Stamatiou, G., Lau, R., Terryn, N., De Rycke, R., Inzé, D., and Berleth, T. (2002). Genetic complexity of CESA gene function in Arabidopsis embryogenesis. Plant Physiol. **130,** 1883–1893.

Birnbaum, K., Shasha, D.E., Wang, J.Y., Jung, J.W., Lambert, G.M., Galbraith, D.W., and Benfey, P.N. (2003). A gene expression map of the Arabidopsis root. Science **302,** 1956–1960.

Boehm, M., and Bonifacino, J.S. (2001). Adaptins: The final recount. Mol. Biol. Cell **12,** 2907–2920.

Breyne, P., Dreesen, R., Vandepoele, K., De Veylder, L., Van Breusegem, F., Callewaert, L., Rombauts, S., Raes, J., Cannoot, B., Engler, G., Inzé, D., and Zabeau, M. (2002). Transcriptome analysis during cell division in plants. Proc. Natl. Acad. Sci. USA **99,** 14825–14830.

Carter, C.J., Bednarek, S.Y., and Raikhel, N.V. (2004). Membrane trafficking in plants: New discoveries and approaches. Curr. Opin. Plant Biol. **7,** 701–707.

Chen, Y.C., and McCormick, S. (1996). Sidecar pollen, an *Arabidopsis thaliana* male gametophytic mutant with aberrant cell divisions during pollen development. Development **122,** 3243–3253.

Cleary, A.L., Gunning, B.E.S., Wasteneys, G.O., and Hepler, P.K. (1992). Microtubule and F-actin dynamics at the division site in living *Tradescantia* stamen hair cells. J. Cell Sci. **103,** 977–988.

Clough, S.J., and Bent, A.F. (1998). Floral dip: A simplified method for *Agrobacterium*-mediated transformation of *Arabidopsis thaliana.* Plant J. **16,** 735–743.

Couchy, I., Bolte, S., Crosnier, M.-T., Brown, S., and Satiat-Jeunemaitre, B. (2003). Identification and localization of a β-COP-like protein involved in the morphodynamics of the plant Golgi apparatus. J. Exp. Bot. **54,** 2053–2063.

Delmer, D.P., and Amor, Y. (1995). Cellulose biosynthesis. Plant Cell **7,** 987–1000.

De Smet, I., Chaerle, P., Vanneste, S., De Rycke, R., Inzé, D., and Beeckman, T. (2004). An easy and versatile embedding method for transverse sections. J. Microsc. (Oxf.) **213,** 76–80.

Desprez, T., Vernhettes, S., Fagard, M., Refrégier, G., Desnos, T., Aletti, E., Py, N., Pelletier, S., and Hofte, H. (2002). Resistance against herbicide isoxaben and cellulose deficiency caused by distinct mutations in same cellulose synthase isoform CESA6. Plant Physiol. **128,** 482–490.

Fagard, M., Desnos, T., Desprez, T., Goubet, F., Refregier, G., Mouille, G., McCann, M., Rayon, C., Vernhettes, S., and Höfte, H. (2000). *PROCUSTE1* encodes a cellulose synthase required for normal cell elongation specifically in roots and dark-grown hypocotyls of Arabidopsis. Plant Cell **12,** 2409–2424.

Fei, H., and Sawhney, V.K. (2001). Ultrastructural characterization of *male sterile33* (*ms33*) mutant in *Arabidopsis* affected in pollen desiccation and maturation. Can. J. Bot. **79,** 118–129.

Friml, J., Benkova, E., Mayer, U., Palme, K., and Muster, G. (2003). Automated whole mount localisation techniques for plant seedlings. Plant J. **34,** 115–124.

Geelen, D., Leyman, B., Batoko, H., Di Sansebastiano, G.P., Moore, I., and Blatt, M.R. (2002). The abscisic acid-related SNARE homolog NtSyr1 contributes to secretion and growth: Evidence from competition with its cytosolic domain. Plant Cell **14,** 387–406.

Geisler-Lee, C.J., Hong, Z., and Verma, D.P.S. (2002). Overexpression of the cell plate-associated dynamin-like GTPase, phragmoplastin, results in the accumulation of callose at the cell plate and arrest of plant growth. Plant Sci. **163,** 33–42.

Gillmor, C.S., Lukowitz, W., Brininstool, G., Sedbrook, J.C., Hamann, T., Poindexter, P., and Somerville, C. (2005). Glycosylphosphatidylinositol-anchored proteins are required for cell wall synthesis and morphogenesis in Arabidopsis. Plant Cell **17,** 1128–1140.

Grini, P.E., Schnittger, A., Schwarz, H., Zimmermann, I., Schwab, B., Jürgens, G., and Hülskamp, M. (1999). Isolation of ethyl methanesulfonate-induced gametophytic mutants in *Arabidopsis thaliana* by a segregation distortion assay using the multimarker chromosome 1. Genetics **151,** 849–863.

Gu, X., and Verma, D.P.S. (1996). Phragmoplastin, a dynamin-like protein associated with cell plate formation in plants. EMBO J. **15,** 695–704.

Hall, Q., and Cannon, M.C. (2002). The cell wall hydroxyproline-rich glycoprotein RSH is essential for normal embryo development in Arabidopsis. Plant Cell **14,** 1161–1172.

Hepler, P.K., and Bonsignore, C.L. (1990). Caffeine inhibition of cytokinesis: Ultrastructure of cell plate formation/degradation. Protoplasma **157,** 182–192.

Hepler, P.K., Vidali, L., and Cheung, A.Y. (2001). Polarized cell growth in higher plants. Annu. Rev. Cell Dev. Biol. **17,** 159–187.

Heslop-Harrison, J. (1987). Pollen germination and pollen-tube growth. Int. Rev. Cytol. **107,** 1–78.

Hong, Z., Bednarek, S.Y., Blumwald, E., Hwang, I., Jurgens, G., Menzel, D., Osteryoung, K.W., Raikhel, N.V., Shinozaki, K., Tsutsumi, N., and Verma, D.P.S. (2003a). A unified nomenclature for *Arabidopsis* dynamin-related large GTPases based on homology and possible functions. Plant Mol. Biol. **53,** 261–265.

Hong, Z., Geisler-Lee, C.J., Zhang, Z., and Verma, D.P.S. (2003b). Phragmoplastin dynamics: Multiple forms, microtubule association and their roles in cell plate formation in plants. Plant Mol. Biol. **53,** 297–312.

Honys, D., and Twell, D. (2004). Transcriptome analysis of haploid male gametophyte development in *Arabidopsis.* Genome Biol. **5,** R85.1–R85.13.

Jefferies, C.J., and Belcher, A.R. (1974). A fluorescent brightener used for pollen tube identification *in vivo.* Stain Technol. **49,** 199–202.

Jürgens, G. (2005a). Plant cytokinesis: Fission by fusion. Trends Cell Biol. **15,** 277–283.

Jürgens, G. (2005b). Cytokinesis in higher plants. Annu. Rev. Plant Biol. **56,** 281–299.

Kang, B.-H., Busse, J.S., and Bednarek, S.Y. (2003a). Members of the Arabidopsis dynamin-like gene family, ADL1, are essential for plant cytokinesis and polarized cell growth. Plant Cell **15,** 899–913.

Kang, B.-H., Busse, J.S., Dickey, C., Rancour, D.M., and Bednarek, S.Y. (2001). The Arabidopsis cell plate-associated dynamin-like protein, ADL1Ap, is required for multiple stages of plant growth and development. Plant Physiol. **126,** 47–68.

Kang, B.-H., Rancour, D.M., and Bednarek, S.Y. (2003b). The dynamin-like protein ADL1C is essential for plasma membrane maintenance during pollen maturation. Plant J. **35,** 1–15.

Karimi, M., De Meyer, B., and Hilson, P. (2005). Modular cloning in plant cells. Trends Plant Sci. **10,** 103–105.

Karimi, M., Inzé, D., and Depicker, A. (2002). GATEWAY™ vectors for *Agrobacterium*-mediated plant transformation. Trends Plant Sci. **7,** 193–195.

Kirchhausen, T., Bonifacino, J.S., and Riezman, H. (1997). Linking cargo to vesicle formation: Receptor tail interactions with coat proteins. Curr. Opin. Cell Biol. **9,** 488–495.

Lane, D.R., et al. (2001). Temperature-sensitive alleles of *RSW2* link the KORRIGAN endo-1,4-β-glucanase to cellulose synthesis and cytokinesis in Arabidopsis. Plant Physiol. **126,** 278–288.

Lauber, M.H., Waizenegger, I., Steinmann, T., Schwarz, H., Mayer, U., Hwang, I., Lukowitz, W., and Jürgens, G. (1997). The *Arabidopsis* KNOLLE protein is a cytokinesis-specific syntaxin. J. Cell Biol. **139,** 1485–1493.

Liu, C.-M., Johnson, S., and Wang, T.L. (1995). *cyd*, a mutant of pea that alters embryo morphology is defective in cytokinesis. Dev. Genet. **16,** 321–331.

Lloyd, C. (1995). Life on a different plane. Curr. Biol. **5,** 1085–1087.

Lukowitz, W., Mayer, U., and Jürgens, G. (1996). Cytokinesis in the Arabidopsis embryo involves the syntaxin-related KNOLLE gene product. Cell **84,** 61–71.

Lukowitz, W., Nickle, T.C., Meinke, D.W., Last, R.L., Conklin, P.L., and Somerville, C.R. (2001). *Arabidopsis cyt1* mutants are deficient in a mannose-1-phosphate guanylyltransferase and point to a requirement of N-linked glycosylation for cellulose biosynthesis. Proc. Natl. Acad. Sci. USA **98,** 2262–2267.

McMahon, H.T., and Mills, I.G. (2004). COP and clathrin-coated vesicle budding: Different pathways, common approaches. Curr. Opin. Cell Biol. **16,** 379–391.

Mineyuki, B., and Gunning, B.E.S. (1990). A role for preprophase bands of microtubules in maturation of new cell walls, and a general proposal on the function of preprophase band sites in cell division in higher plants. J. Cell Sci. **97,** 527–537.

Mineyuki, Y. (1999). The preprophase band of microtubules: Its function as a cytokinetic apparatus in higher plants. Int. Rev. Cytol. **187,** 1–50.

Müller, I., Wagner, W., Völker, A., Schellmann, S., Nacry, P., Küttner, F., Schwarz-Sommer, Z., Mayer, U., and Jürgens, G. (2003). Syntaxin specificity of cytokinesis in *Arabidopsis.* Nat. Cell Biol. **5,** 531–534.

Nickle, T.C., and Meinke, D.W. (1998). A cytokinesis-defective mutant of *Arabidopsis* (*cyt1*) characterized by embryonic lethality, incomplete cell walls, and excessive callose accumulation. Plant J. **15,** 321–332.

Nicol, F., His, I., Jauneau, A., Vernhettes, S., Canut, H., and Höfte, H. (1998). A plasma membrane-bound putative endo-1,4-β-D-glucanase is required for normal wall assembly and cell elongation in *Arabidopsis.* EMBO J. **17,** 5563–5576.

Odell, J.T., Hoopes, J.L., and Vermerris, W. (1994). Seed-specific gene activation mediated by the Cre/*lox* site-specific recombination system. Plant Physiol. **106,** 447–458.

Pagant, S., Bichet, A., Sugimoto, K., Lerouxel, O., Desprez, T., McCann, M., Lerouge, P., Vernhettes, S., and Höfte, H. (2002). *KOBITO1* encodes a novel plasma membrane protein necessary for normal synthesis of cellulose during cell expansion in Arabidopsis. Plant Cell **14,** 2001–2013.

Palevitz, B.A. (1980). Comparative effects of phalloidin and cytochalasin-B on motility and morphogenesis in Allium. Can. J. Bot. **58,** 773–785.

Peng, L., Hocart, C.H., Redmond, J.W., and Williamson, R.E. (2000). Fractionation of carbohydrates in *Arabidopsis* root cell walls shows that three radial swelling loci are specifically involved in cellulose production. Planta **211,** 406–414.

Pickert, M. (1988). *In vitro* germination and storage of trinucleate *Arabidopsis thaliana* (L.) pollen grains. Arabidopsis Inf. Serv. **26,** 39–42.

Praefcke, G.J.K., and McMahon, H.T. (2004). The dynamin superfamily: Universal membrane tubulation and fission molecules? Nat. Rev. Mol. Cell Biol. **5,** 133–147.

Samuels, A.L., Giddings, T.H., Jr., and Staehelin, L.A. (1995). Cytokinesis in tobacco BY-2 and root tip cells: A new model of cell plate formation in higher plants. J. Cell Biol. **130,** 1345–1357.

Sanderfoot, A.A., Pilgrim, M., Adam, L., and Raikhel, N.V. (2001). Disruption of individual members of Arabidopsis syntaxin gene families indicates each has essential functions. Plant Cell **13,** 659–666.

Sano, T., Higaki, T., Oda, Y., Hayashi, T., and Hasezawa, S. (2005). Appearance of actin microfilament 'twin peaks' in mitosis and their function in cell plate formation, as visualized in tobacco BY-2 cells expressing GFP-fimbrin. Plant J. **44,** 595–605.

Schrick, K., Mayer, U., Horrichs, A., Kuhnt, C., Bellini, C., Dangl, J., Schmidt, J., and Jürgens, G. (2000). FACKEL is a sterol C-14 reductase required for organized cell division and expansion in *Arabidopsis* embryogenesis. Genes Dev. **14,** 1471–1484.

Torres-Ruiz, R.A., and Jürgens, G. (1994). Mutations in the FASS gene uncouple pattern formation and morphogenesis in Arabidopsis development. Development **120,** 2967–2978.

Traas, J., Bellini, C., Nacry, P., Kronenberger, J., Bouchez, D., and Caboche, M. (1995). Normal differentiation patterns in plants lacking microtubular preprophase bands. Nature **375,** 676–677.

Twell, D., Yamaguchi, J., and McCormick, S. (1990). Pollen-specific gene expression in transgenic plants: Coordinate regulation of two different tomato gene promoters during microsporogenesis. Development **109,** 705–713.

Ursin, V.M., Yamaguchi, J., and McCormick, S. (1989). Gametophytic and sporophytic expression of anther-specific genes in developing tomato anthers. Plant Cell **1,** 727–736.

Van Aelst, A.C., Pierson, E.S., Van Went, J.L., and Cresti, M. (1993). Ultrastructural changes of *Arabidopsis thaliana* pollen during final maturation and rehydration. Zygote **1,** 173–179.

Van Damme, D., Bouget, F.-Y., Van Poucke, K., Inzé, D., and Geelen, D. (2004a). Molecular dissection of plant cytokinesis and phragmoplast structure: A survey of GFP-tagged proteins. Plant J. **40,** 386–398.

Van Damme, D., Van Poucke, K., Boutant, E., Ritzenthaler, C., Inzé, D., and Geelen, D. (2004b). In vivo dynamics and differential microtubule-binding activities of MAP65 proteins. Plant Physiol. **136,** 3956–3967.

Vanstraelen, M., Van Damme, D., De Rycke, R., Mylle, E., Inzé, D., and Geelen, D. (2006). Cell cycle dependent targeting of a kinesin at the plasma membrane demarcates the division site in plant cells. Curr. Biol. **16,** 308–314.

Völker, A., Stierhof, Y.-D., and Jürgens, G. (2001). Cell cycle-independent expression of the *Arabidopsis* cytokinesis-specific syntaxin KNOLLE results in mistargeting to the plasma membrane and is not sufficient for cytokinesis. J. Cell Sci. **114,** 3001–3012.

Wick, S.M. (1991). Spatial aspects of cytokinesis in plant cells. Curr. Opin. Cell Biol. **3,** 253–260.

Williamson, R.E., Burn, J.E., Birch, R., Baskin, T.I., Arioli, T., Betzner, A.S., and Cork, A. (2001). Morphology of *rsw1*, a cellulose-deficient mutant of *Arabidopsis thaliana.* Protoplasma **215,** 116–127.

Yoneda, A., Akatsuka, M., Kumagai, F., and Hasezawa, S. (2004). Disruption of actin microfilaments causes cortical microtubule disorganization and extra-phragmoplast formation at M/G_1 interface in synchronized tobacco cells. Plant Cell Physiol. **45,** 761–769.

Zuo, J., Niu, Q.-W., Nishizawa, N., Wu, Y., Kost, B., and Chua, N.-H. (2000). KORRIGAN, an Arabidopsis endo-1,4-β-glucanase, localizes to the cell plate by polarized targeting and is essential for cytokinesis. Plant Cell **12,** 1137–1152.

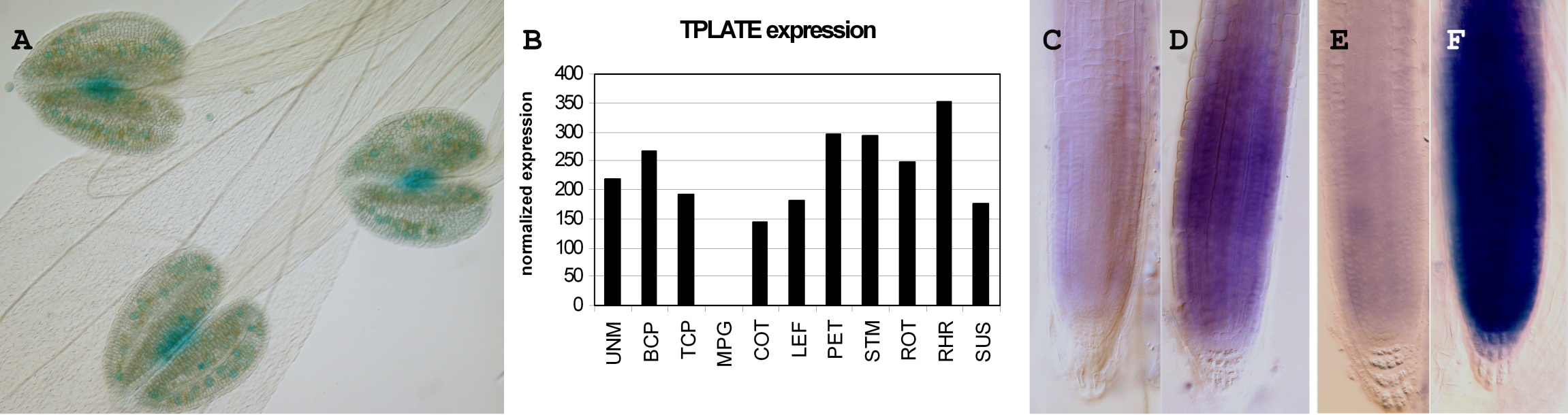

Figure S1: Expression data of TPLATE
(A) TPLATE genomic-GUS expression in the connectivum that connects the anther to the filament and in pollen grains. (B) Normalized data of gametophytic and sporophytic expression of TPLATE in different tissues as analyzed by Honys and Twell, 2004. Expression signal 0 means that the detection call value was not present in all replicates tested. UNM: uninucleate microspores; BCP: bicellular pollen; TCP: immature tricellular pollen; MPG: mature pollen grain; COT: open cotyledon stage; LEF: leaves; PET: petiole; STM: stem; ROT: roots; RHR: root hair zone; SUS: suspension cells. (C, D, E and F) Whole mount in situ hybridization of Arabidopsis Col-0 (C,D) and 35S::TPLATE-GFP roots (E,F) using sense (C,E) and antisense probe (D, F) against TPLATE. In wild-type Col-0 background, the antisense probe signal is present throughout the root meristem, although not uniformly distributed, with the lowest level of expression at the very tip and a stronger expression near the elongation zone.

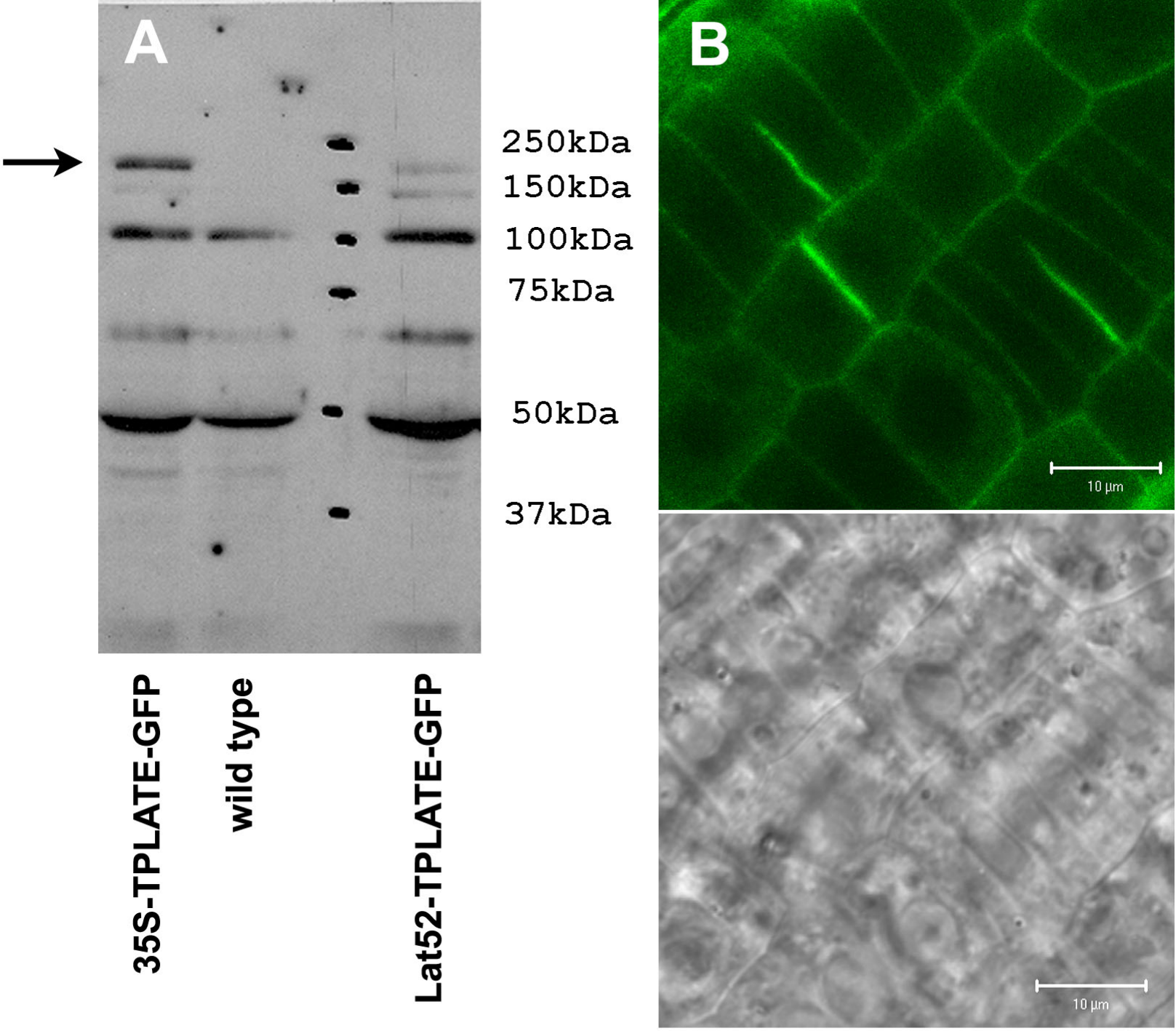

Figure S2: Ectopic expression of Lat52-TPLATE-GFP
(A) Western blot of Arabidopsis seedlings with anti-GFP antibody showing a 160kDa band (arrow) of TPLATE-GFP in 35S-TPLATE-GFP over-expressing plants (lane 1) and Lat52-TPLATE-GFP expressing plants (lane 3) while the band is absent in wild-type plants (lane 2). (B) Confocal image through the root of an Arabidopsis plant transformed with Lat52-TPLATE-GFP showing cell plate labeling of TPLATE-GFP. Bars equal 10µm.

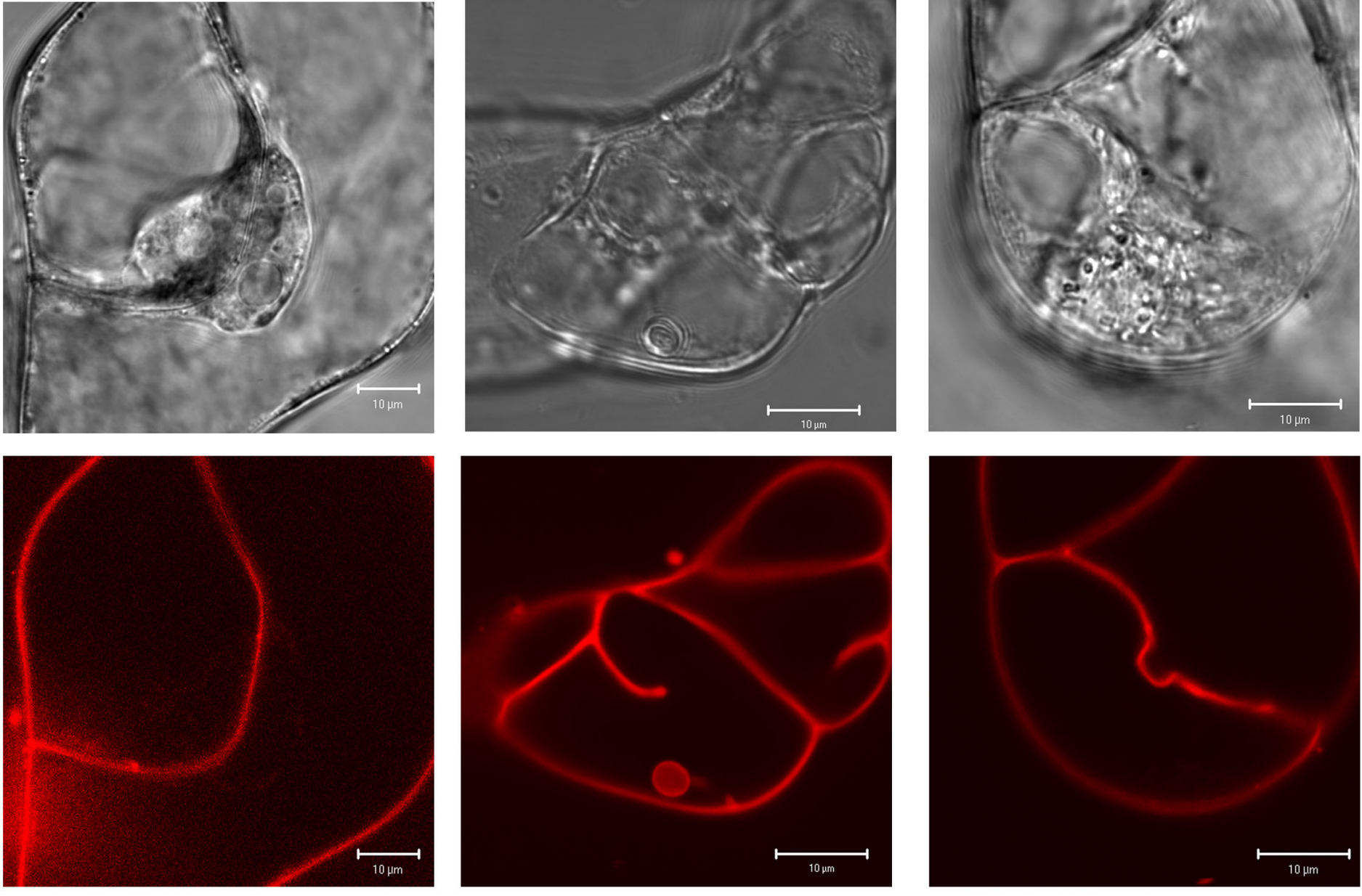

Figure S3: RNAi effects in BY-2
Confocal sections of PI stained cell plate aberrations in BY-2 cells transformed with the pH7GWIWG(II) vector containing the tobacco TPLATE TAG BSTT43-4-330. Bars equal 10µm.

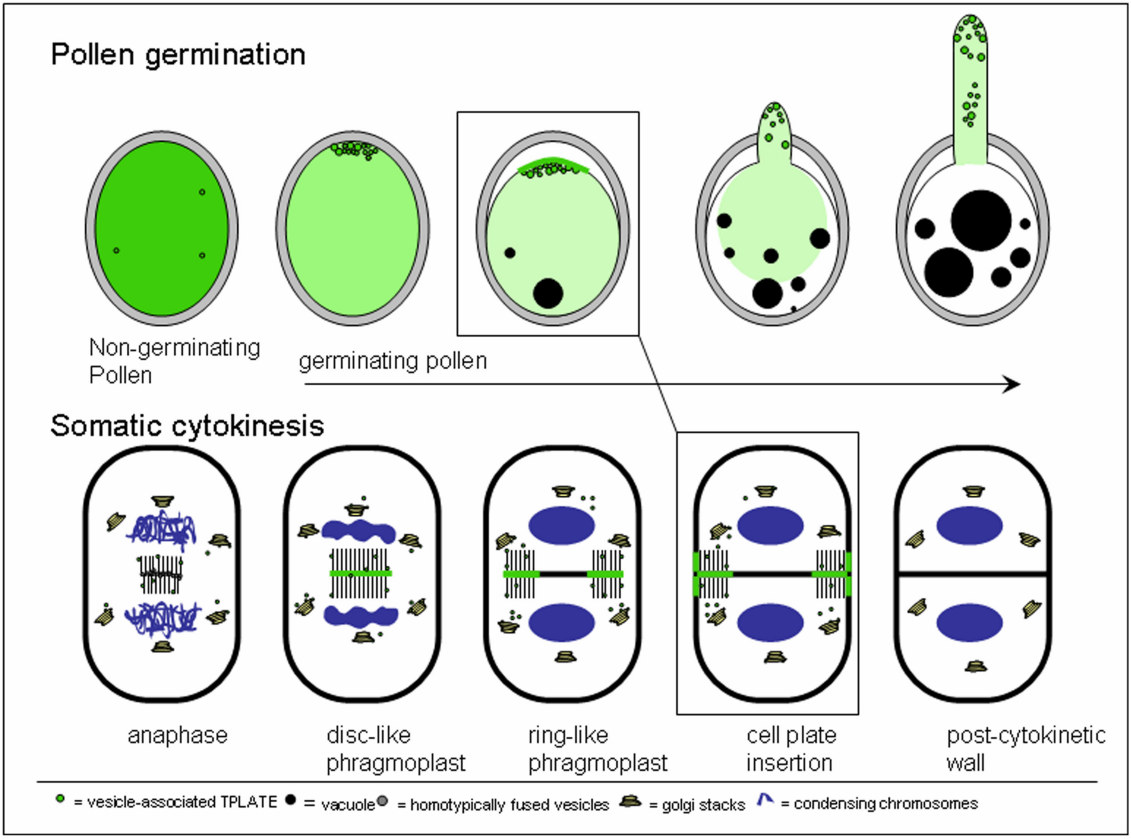

Figure S4: Model of TPLATE function in pollen germination and in somatic cytokinesis
Mature pollen is stacked with vesicles while the vacuolar compartment is negligible compared to, for example, a cortex cell. Upon rehydration, the vesicles change in composition and concentrate at the cell periphery (Van Aelst et al., 1993). In rehydrated pollen, TPLATE GFP accumulates at the pollen tube exit site where the future pollen tube is formed. Small vacuoles reunite to make larger compartments and provide turgor pressure for tube expansion. TPLATE moves into the pollen tube tip during pollen tube formation. During somatic cytokinesis, Golgi- or endosomal derived vesicles are transported to the phragmoplast midzone where they fuse. TPLATE GFP concentrates at the midzone and follows the leading edges of the expanding cell plate (Van Damme et al., 2004a). During cell- plate mother-wall contact, TPLATE GFP accumulates at a narrow zone surrounding the cortical insertion site. This is a unique property of TPLATE not observed for other cell plate associated proteins studied so far (Demidov et al., 2005; Gu and Verma, 1996; Heese et al., 2001; Ingouff et al., 2005; Lauber et al., 1997; Lee et al., 2001; Nishihama et al., 2001; Peterman et al., 2004; Van Damme et al., 2004a; Vanstraelen et al., 2004). As soon as the cell plate is inserted into the mother wall, TPLATE GFP dissociates from the division zone and the cell plate. The communality of pollen germination and final step of cytokinesis is the site specific plasma membrane targeting of vesicles.

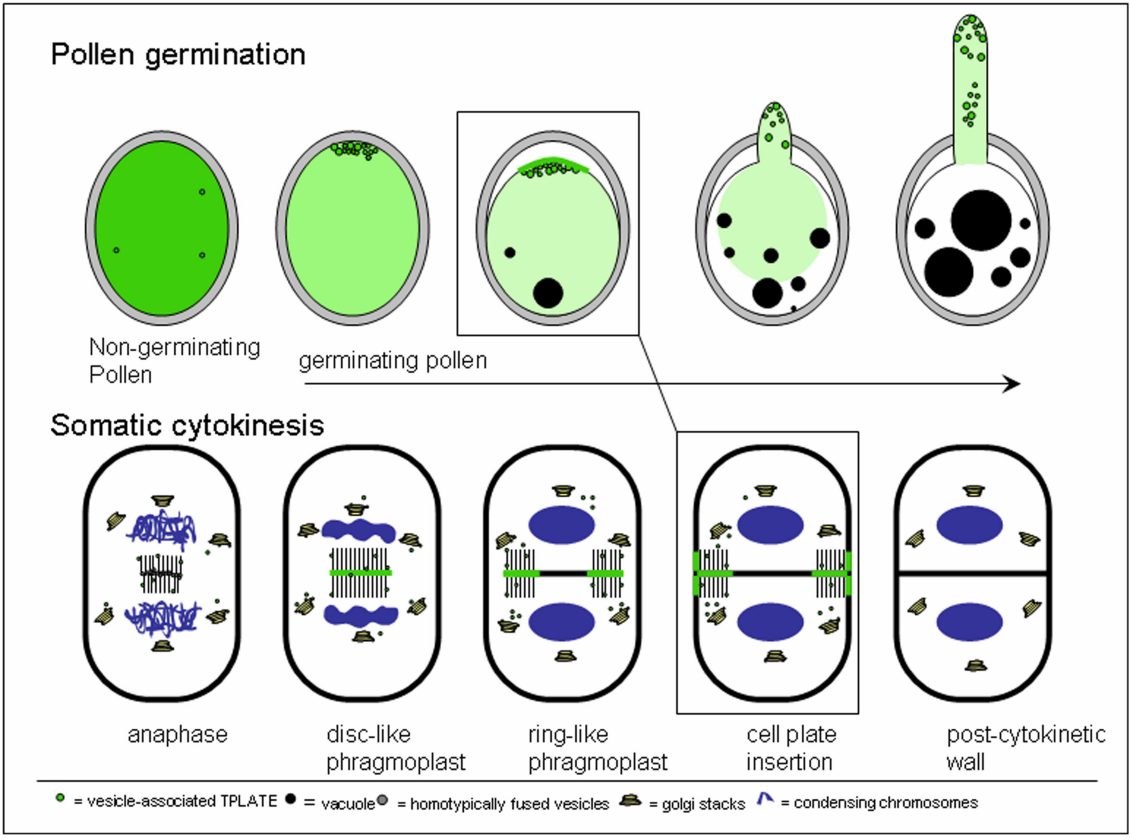

Figure S5: Model of TPLATE function in pollen germination and in somatic cytokinesis
Mature pollen is stacked with vesicles while the vacuolar compartment is negligible compared to, for example, a cortex cell. Upon rehydration, the vesicles change in composition and concentrate at the cell periphery (Van Aelst et al., 1993). In rehydrated pollen, TPLATE GFP accumulates at the pollen tube exit site where the future pollen tube is formed. Small vacuoles reunite to make larger compartments and provide turgor pressure for tube expansion. TPLATE moves into the pollen tube tip during pollen tube formation. During somatic cytokinesis, Golgi- or endosomal derived vesicles are transported to the phragmoplast midzone where they fuse. TPLATE GFP concentrates at the midzone and follows the leading edges of the expanding cell plate (Van Damme et al., 2004a). During cell- plate mother-wall contact, TPLATE GFP accumulates at a narrow zone surrounding the cortical insertion site. This is a unique property of TPLATE not observed for other cell plate associated proteins studied so far (Demidov et al., 2005; Gu and Verma, 1996; Heese et al., 2001; Ingouff et al., 2005; Lauber et al., 1997; Lee et al., 2001; Nishihama et al., 2001; Peterman et al., 2004; Van Damme et al., 2004a; Vanstraelen et al., 2004). As soon as the cell plate is inserted into the mother wall, TPLATE GFP dissociates from the division zone and the cell plate. The communality of pollen germination and final step of cytokinesis is the site specific plasma membrane targeting of vesicles.